

ORE MINERALOGY AND FLUID INCLUSION STUDY
OF THE
SOUTHERN AMETHYST VEIN SYSTEM,
CREEDE MINING DISTRICT, COLORADO

by

Richard W. Robinson

Submitted in Partial Fulfillment
of the Requirements for the Degree of
Master of Science in Geology

New Mexico Institute of Mining and Technology

Socorro, New Mexico

May 1981

ACKNOWLEDGMENTS

I would like to thank Paul Eimon, of Chevron Resources Company, who was instrumental in my involvement in the Creede area. His professional advice and enthusiasm have been invaluable to me.

This work has benefitted greatly from the helpful guidance and stimulating discussions with my academic advisors Dr. David Norman, Dr. Philip Behtke, and Dr. Marc Bodine. The detailed editing of this paper by Dave Norman has greatly improved this text.

Financial support and permission of access to the property by Minerals Engineering Company and Chevron Resources Company were essential to this work and are warmly appreciated. Interest expressed by John Beeder of Minerals Engineering in this thesis has been of great value.

My association with the exploration activities of Chevron Resources Company, directed by Paul Eimon, was concurrent with the field studies of this thesis. Of the many geologists who were involved with this exploration activity, I would especially like to thank Phil Giudice, John Rice, and Bruce Surgenor for all of their contributions.

The geologic framework and many of the ideas upon which this paper is based are the result of the work of the U. S.

Geological Survey. My association with the distinguished researchers of the survey benefited this thesis greatly.

The contributions of my fellow graduate students at New Mexico Institute of Mining and Technology were a constant help to me during the course of this study. I am especially indebted to Carl Bernhardt, whose unselfish investment of time and patience enabled me to gain an understanding of geothermal systems and processes that was essential to the interpretations of the data in this thesis.

I would like most of all to thank my wife Carol, for without her love and enthusiastic attitude this thesis would never have been worthwhile. Finally, it is necessary to acknowledge He who ultimately created the material upon which this thesis is based.

ABSTRACT

The Creede mining district in southwestern Colorado has been the subject of many studies in recent years. A large number of these studies have concentrated on the OH vein. One of the most productive areas in the past was the southern Amethyst vein system, however this area has received limited attention in the study of the district. Therefore, field studies, which included detailed mapping and sampling, were performed on the southern Amethyst vein system, as well as studies of the paragenesis, mineralogy, and fluid inclusions.

The mineralization in the southern Amethyst vein system occurs as sulfides in veins and disseminated in the volcanic host rocks. All of the mineralization, both vein and disseminated, is confined to areas of high fracture density and brecciation in the Campbell Mountain ash flow tuff unit which forms the hanging wall, and also the footwall in places, of the Amethyst fault. The mineralization in the southern Amethyst vein system is fine grained, usually less than 100 μ in diameter. Zones up to 200m in a single dimension of disseminated mineralization occur in brecciated rock that has been filled by clear quartz and < 3.9% sulfides. The precious metal values in these disseminated ore zones are remarkably consistent, but the amount of this type of mineralization in the southern Amethyst system is not known.

The paragenesis was studied to determine when silver mineralization occurred. The paragenesis is divided into two stages. Stage 1 is a sulfide poor assemblage characterized by rhodochrosite, quartz, barite, and an absence of silver. Stage 2 is a complex stage made up of three substages. Substage A contains amethyst, white and clear quartz, base metal sulfides, and no silver. Substage B contains amethyst, barite, base metal sulfides, and silver bearing copper sulfides. Substage C contains amethyst, white and clear quartz, copper sulfides bearing no silver, base metal sulfides, iron and manganese oxides, acanthite, tetrahedrite, and native silver. Crosscutting relationships among the substages are vague. Silver occurs in economic quantities in the two later substages of stage 2. Veins containing stage 1 material are found only in the lower levels of the study area, whereas stage 2 veins occur throughout the southern Amethyst system. Disseminated mineralization appears to be related to substage C of stage 2, but no direct physical link was found to exist between disseminated and vein ore material. All of the mineralization in the southern Amethyst vein system occurred early in the paragenesis of the Creede ores that has been summarized in recent studies of the district.

Fluid inclusion analysis of vein quartz from the lower levels of the mine had average homogenization temperatures of 238°C and salinities of 9.5 eq. wt. % NaCl. Analysis from the top levels of the mine had average homogenization

temperatures of 170°C and average salinities of 6.5 eq. wt. % NaCl. Several inclusions from the upper levels of the mine showed evidence of containing high amounts of CO₂ and/or CH₄. The presence of these gases was interpreted as indirect evidence that boiling of the ore fluids may have occurred. Very limited amounts of intense sericitic alteration, which is associated with zones of boiling on the OH vein, were found in the study area.

Enthalpy values calculated from the fluid inclusion analysis done in this study show linear relationships when plotted against both salinity and elevation. When such linear relationships are found in active geothermal areas it is interpreted to indicate that mixing of hot (hydrothermal) waters and cooler (shallow) waters has occurred. Therefore a mixing model is proposed for the southern Amethyst vein system at the time of mineralization. Fluids flowing laterally along the top of a freely convecting hydrothermal cell, as proposed in several recent studies, encountered cooler dilute waters in the southern portion of the vein system. These two fluids mixed, with the degree of mixing decreasing with depth. Mixing caused rapid dilution and cooling of the ore fluids which resulted in rapid deposition of base and precious metals from solution. Large zones of disseminated ore with consistent metal contents that occur at shallow depths (within 200m of the present surface) are the most significant result of this proposed mixing model.

TABLE OF CONTENTS

	Page
LIST OF ILLUSTRATIONS	ix
INTRODUCTION AND GEOLOGIC FRAMEWORK	1
Geology and Geologic History	4
Mineralization	5
Chemical Environment of Mineralization	6
Hydrothermal Model	6
Methods of Investigation	8
RESULTS	9
Vein Mineralization	9
Paragenesis	14
Disseminated Mineralization	19
Distribution and Interrelationships of Vein and Disseminated Mineralization	20
Alteration	23
Fluid Inclusion Analysis	23
CO ₂ and/or CH ₄ Rich Inclusions	29
DISCUSSION	33
Mineralogy and Paragenesis	33
Decrease of Homogenization Temperature	36
Enthalpy of Fluids	37
Chemical Controls on the Properties of Mineralization	43
Surface Reconstruction	45
SUMMARY AND CONCLUSIONS	46
Characteristics of Mineralization	46
Application to Proposed Hydrothermal Models	50
Future Research	52
APPENDIX A: Fluid Inclusion Data and Sample Locations	53
APPENDIX B: Comparison of Creede to Other Geothermal Systems	70

REFERENCES 78

LIST OF ILLUSTRATIONS

Figure	Page
1. Location Maps for the Creede Mining District . . .	3
2. Generalized Paragenesis of Major Ore and Gangue Minerals	12
3. Longitudinal Projection of Amethyst-OH Veins .	16
4. Plot of Elevation vs. Homogenization Temperature of Fluids	26
5. Plot of Elevation vs. Salinity of Fluids . . .	28
6. Salinity vs. Homogenization Temperature on Representative Mine Levels	31
7. Summary of the Paragenesis of Creede ores . .	35
8. Plot of Elevation vs. Enthalpy of Fluids . .	39
9. Plot of Enthalpy vs. Salinity of Fluids . . .	42
10. Proposed Model of Mixing	48

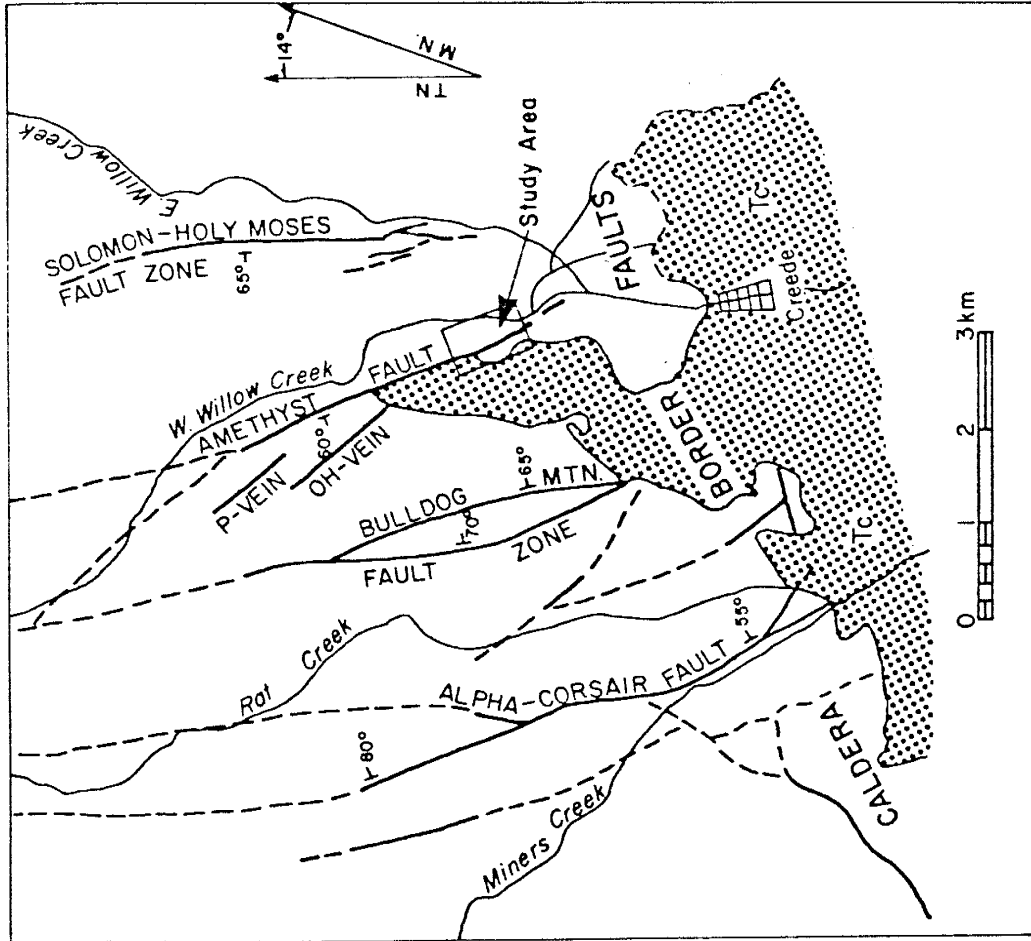
INTRODUCTION AND GEOLOGIC FRAMEWORK

The Creede mining district is located in the central San Juan Mountains in southwestern Colorado. Significant amounts of Ag-Pb-Zn-Cu-Au ores have been produced from the district for nearly 100 years. The Creede district has been the subject of an intensive study by the U.S. Geological Survey to determine the geologic, hydrologic, and chemical environment of deposition of the ores. The results of these studies are being published as a continuing series in *Economic Geology*, (Steven and Eaton, 1975; Bethke et.al., 1976; Barton et.al., 1977; Bethke and Rye, 1979). These studies have concentrated, due to access restrictions, mainly on the OH vein and much of the rest of the district, including the southern Amethyst vein system, has received limited recent attention. This southern portion of the vein system has been one of the most productive areas in the past, and recent drilling and sampling indicates that it contains significant quantities of disseminated mineralization for possible future production. Therefore the southern one-third of the Amethyst vein system was chosen as an area for study. This study included detailed mapping and sampling, determination of the mineralogy and paragenesis of the vein and disseminated mineralization, and fluid inclusion analysis of vein material.

Fig. 1. Location maps for the Creede mining district and for the study area near the southern end of the Amethyst vein system, modified from Steven and Eaton (1975).

Calderas shown are: S, Silverton; LC, Lake City; Bz, Bonanza; SM, Summitville; P, Platoro; LG, La Garita; SL, San Luis; B, Bachelor; C, Creede. Faults shown are only those that were active just before and during mineralization.

FAULTS AND VEINS IN THE CREEDE MINING DISTRICT



EXPLANATION



Creede Fm.



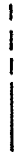
Undivided volcanics



70°

FAULT WITH DIP

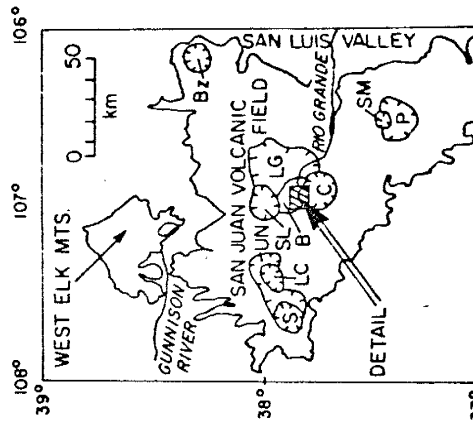
Dashed Where Approx.



CONTACT

Dashed Where Approx.

SAN JUAN VOLCANIC FIELD CALDERAS



Geology and Geologic History

The Creede district is located in a cluster of at least five late Oligocene calderas (fig. 1). The geologic history of the San Juan Mountains has been documented by Lipman et.al. (1970) and Steven and Lipman (1976). Volcanic activity began in early Oligocene time with the eruption of andesitic lavas from many widespread centers. These volcanos were especially active between 30 and 35 m.y. ago, and they formed a major volcanic field that covered most of the southern Rocky Mountains, (Steven and Epis, 1968; Steven, 1975). The San Juan Mountains are the largest remaining portion of that field (fig. 1). These andesitic lavas in the Creede area were probably erupted directly onto Precambrian basement rocks, (Lipman et.al., 1970).

Following the andesitic lavas were a series of quartz latitic to rhyolitic ash flows erupted between 26 and 28 m.y. ago. The calderas associated with the ash flows in the Creede district are from oldest to youngest: La Garita, Bachelor, San Luis, and Creede. Between 25 and 23 m.y. ago the character of the erupted volcanics changed from quartz latite and low silica rhyolite to a bimodal assemblage of basalts and high silicic alkali rhyolites which has been dominant ever since (Lipman et.al., 1970).

Mineralization

The age of mineralization at Creede has been dated at 24.6 +/- 0.6 m.y. (Bethke et.al., 1976). This places the hydrothermal event responsible for the Creede ores approximately 2 m.y. later than the youngest known volcanic activity (dated at 26.4 +/- 0.6 m.y.) in the area. These authors conclude that hydrothermal activity may have been related to either a late intrusion associated with the last volcanic event in the district or to an early intrusion related to the bimodal basalt-silicic rhyolite assemblage.

Repeated collapse and resurgence in the cluster of nested calderas in which the Creede district is located makes the volcano-tectonic history of the district very complex. A keystone graben was formed during resurgent doming of the Bachelor Mountain caldera. The fractures associated with this keystone graben were reactivated after the Creede caldera had formed (Steven and Ratte, 1960, 1965). Mineralization was controlled by these reactivated fractures. The keystone graben occurs in the rhyolitic ash flow tuffs of the intra-caldera Bachelor Mountain member of the Carpenter Ridge tuff, Ratte and Steven (1967). The Bachelor Mountain member is composed of the lower, blue-grey-to-red, densely welded, fluidal Willow Creek tuff, the intermediate, purple-to-pink, eutaxitic-to-vitroclastic, compactly welded Campbell Mountain tuff, and the upper soft, poorly welded to unwelded Windy Gulch tuff. The fractures

of the graben are terminated where they intersect the north margin of the Creede caldera.

Chemical Environment of Mineralization

Barton et.al. (1977) documented the chemical environment of deposition of the ores in the OH vein. Briefly summarized, they conclude that the environment of ore deposition had the following characteristics: (1) temperature of 250°C, (2) pressure of about 50 bars (the fluids were boiling near the top of the ore zone), (3) pH of 5.4, (4) salinity of about 1 molal (4 to 12 eq. wt. % NaCl), and (5) total concentration of sulfur in solution of approx. 0.02 molal. The activities of oxygen and sulfur varied considerably during ore deposition. Most of the ore deposition occurred from sulfate- rather than sulfide-rich solutions, and there were recurrent departures from redox equilibrium among the aqueous sulfur species. Geochemical studies of the carbonates of Amethyst and Bulldog fault zones indicates that the chemical environment summarized above probably prevailed district-wide during the mineralizing event(s).

Hydrothermal Model

A model for the hydrothermal system responsible for ore deposition at Creede was first proposed by Steven and Eaton (1975), and was later modified by Barton et.al. (1977) and Bethke and Rye (1979). A stock is postulated to have been emplaced beneath the Bachelor caldera approx. 24.6 m.y.

ago. The pressure from the stock reactivated the keystone graben of the Bachelor caldera and also started a deeply circulating hydrothermal system as part of a cooling process. The ores were deposited from this freely convecting hydrothermal system that, according to stable isotope data by Bethke and Rye (1979), was charged largely by meteoric waters (from two different sources) and with lesser amounts of magmatic waters. Lead isotope evidence (Doe et.al., 1979) indicates that the lead in Creede ores had its source in Precambrian basement rocks, or in sediments derived from them, which are postulated to underlie the volcanics in the area. The source of the other metals, salts, and sulfur that were in the ore solutions is not known. The circulating system deposited gangue and ore minerals near the top of the convecting cell in a hypogene enrichment process that extracted metals and sulfur from whatever sources were available at depth and swept them toward the surface. The flow direction in the cell was from north to south along the top of the cell. The solutions convected downward at the southern end of the fracture system upon encountering the ring fracture zone of the Creede caldera. Boiling, with loss of acid components which recondensed in the cooler overlying rocks, was responsible for the formation of an intensely altered sericitic "cap" above the ore. Precipitation of ore minerals is attributed to cooling and to a rise in pH due to the loss of acid constituents through boiling (Barton et.al., 1977).

Methods of Investigation

The study area was mapped and sampled in detail during spring, 1979, and summer, 1980. Surface exposure is poor in the mineralized portions of the district, so virtually all mapping and sampling was performed underground (fig. 2). Samples of ore material came from veins exposed underground and in drill core. These samples were examined with a scanning electron microscope and by reflected light microscopy. Fluid inclusions were analyzed on a Linkam TH-600 heating and freezing stage.

RESULTS

Vein Mineralization

The Amethyst vein system is a complex series of faults and veins. These veins vary from less than 0.01m to over 5m in width in the southern one-third of the system. Common structural features displayed in the system include warped fault planes, anastomosing veins (net-like appearance), cymoid loops, and multiple periods of movement along the same structure. The main vein of the system is the Amethyst vein. It is 1m to 6m wide, dips 60° to 80° southwest, and strikes approximately N20 W in the study area. The vein material occupies open space left by extensional movement which occurred prior to mineralization. Normal dip-slip movement of this fault was a minimum of 550 meters. Just to the south of the study area this vein bends sharply to the southeast and becomes a mass of horsetail fractures near the junction of West and East Willow Creeks.

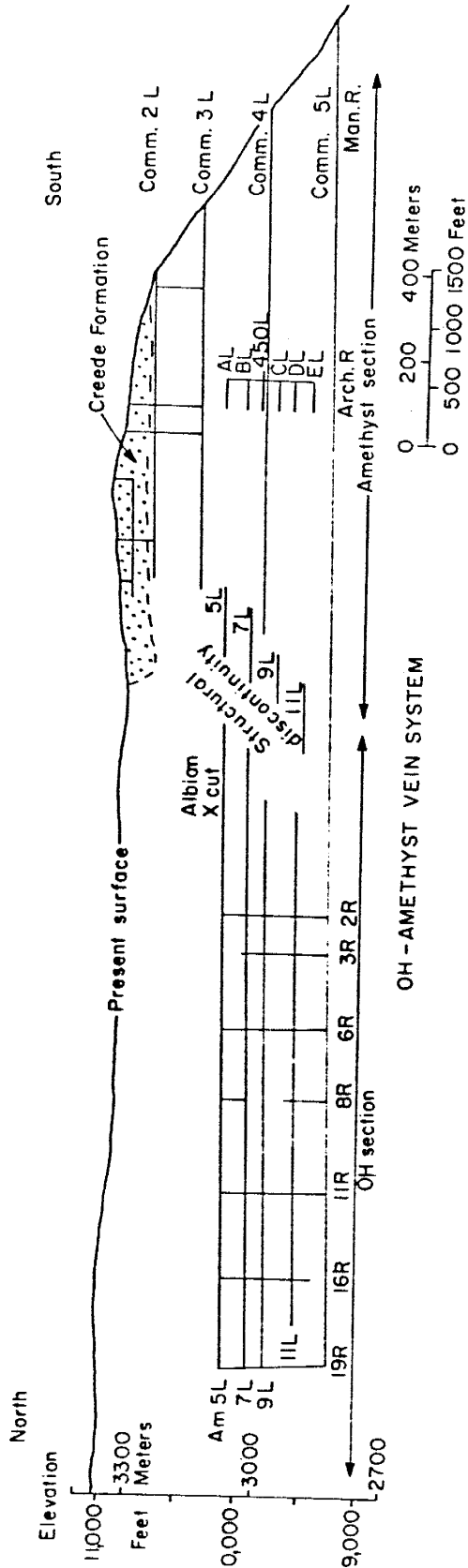
There are no known major veins that split off from the Amethyst fault in the study area, although there are numerous small veins that split off from the Amethyst fault and these are associated with changes in dip and strike along the fault plane. One large cymoid-type loop is present in the form of the Ancestral Amethyst fault-and-vein which was first mapped by Steven and Ratte (1965), however movement along the Ancestral Amethyst fault is believed to have taken place approximately 2 m.y. prior to

mineralization. Therefore it is not considered to be a major split as are the OH and P veins.

The Amethyst vein and the Ancestral Amethyst fault can be traced between levels and for long distances along strike. This is due to the large size of these structures and to the large amount of movement associated with major faulting along them. With the exception of these two large structures, there were no veins that could be traced between levels or for any significant distance along strike in the study area. This is because these smaller veins (1cm to 30cm wide) show tendencies to display marked rolls in their dips, variations in strike, pinching and swelling over short distances, numerous splits, etc., which prevented attempts to trace them. Displacement along the majority of these smaller veins appears to be insignificant. Mineralization post-dates movement in nearly all veins. Evidence of this is the lack of crushed material in the veins, sharp wallrock-vein contacts, euhedral crystals growing toward the center of veins, symmetrical mineralogic banding, and matching wallrock surfaces. Both the Amethyst and Ancestral Amethyst faults-and-veins show some evidence of post ore movement, but this movement was probably not significant.

The vein mineralization is fine grained, generally less than 150u. Three vein mineral assemblages were recognized in the study area. These mineral assemblages were defined as minerals that occur together spacially and therefore

Fig. 2. Generalized longitudinal projection, looking east, onto a vertical plane of the OH and southern Amethyst vein. Modified from Barton and others (1977). The wall rock of these veins is welded ash flow tuffs of the Campbell Mountain unit of the Carpenter Ridge Tuff, except for the fluvial Creede Formation where it is shown. Several main levels are shown from the OH and Amethyst veins. The Amethyst vein workings extend approx. 2 km beyond the "structural discontinuity" but are not shown here. Samples for analysis came from E, D, C, Commodore 4, and the 450 level on the Archimedes Raise, from drill core above and below Commodore 2 level, and from Commodore 2 level. All workings between the 450 level and Commodore 2 level were inaccessible during the study.



OH - AMETHYST VEIN SYSTEM

were useful as aids in field mapping. All of the following assemblages were hypogene in origin.

The first assemblage consists of quartz, rhodochrosite, barite, galena, sphalerite, pyrite, chalcopyrite, and minor amounts of covellite and calcite. The quartz in this assemblage is white, grey, green, or clear. No amethyst colored quartz is associated with this assemblage. Small amounts of the the clay minerals smectite and illite were found in this assemblage at the vein-wallrock contact.

The second assemblage includes quartz, barite, galena, sphalerite, pyrite, chalcopyrite, chalcocite, covellite, acanthite, tetrahedrite, native silver, several unidentified sulfosalts, and suspected alabandite. Silver was found in the following minerals, listed in order of decreasing amount of silver; acanthite, tetrahedrite, covellite, chalcocite, and chalcopyrite. No quantitative measurement was made of the amount silver in the above minerals. Much of the quartz was amethystine, with variable shades of purple. There was also more minor amounts of clear to white quartz than was present in the first assemblage. Several intergrown clays are associated with this assemblage including smectite, illite, and minor amounts of kaolinite.

The third mineral assemblage is composed of quartz, hematite, undivided manganese oxides, native silver, and very minor amounts of acanthite, pyrite, and galena. The quartz in this assemblage is white to clear with rare purple

shading. Silver was found as acanthite and as native silver. The iron and manganese oxides show fine banding with intergrown quartz and distinct colloform textures. Clay minerals found in this assemblage are kaolinite and smectite.

Paragenesis

The paragenesis was studied in order to gain an understanding of the temporal relationship of silver mineralization relative to the other mineralization in the study area. The paragenetic stages are defined temporally and are composed of the spatially defined mineral assemblages described above. The paragenesis has been divided into two main stages (fig. 3). The temporal relationship between these two stages is clear because stage 1 veins are crosscut by veins of stage 2 where both stages are exposed together. Stage 2, however, is actually a complex stage with three substages within this single main stage. These three substages appear to be closely related both temporally and spatially.

Stage 1 is made up of the minerals from the first assemblage mentioned above (fig. 3). No common silver bearing minerals such as acanthite, tetrahedrite, or native silver were found in this stage, nor was silver detected in any other mineral in this stage. Several replacement textures and textures indicating successive deposition,

Fig. 3. Generalized paragenesis of the major ore and gangue minerals in the southern one-third of the Amethyst vein system.

MINERAL

STAGE 1

STAGE 2

	Substage A	Substage B	Substage C
Rhodochrosite	_____		
Amethyst	_____	_____	_____
White quartz	_____	_____	_____
Clear quartz	_____	_____	_____
Barite	_____	_____	_____
Calcite	_____	_____	_____
Sphalerite	_____	_____	_____
Galena	_____	_____	_____
Pyrite	_____	_____	_____
Chalcopyrite	_____	_____	_____
Covellite	_____	_____	_____
Chalcocite	_____	_____	_____
Hematite	_____	_____	_____
Pyrolusite	_____	_____	_____
Tetrahedrite	_____	_____	_____
Native silver	_____	_____	_____
Acanthite	_____	_____	_____
Alabandite	_____	_____	_____

according to Edwards (1947), were common among the sulfide minerals. These textures included straight crystal boundaries with internal angles $<180^\circ$, transecting veins, relict crystal form of pseudomorphed minerals, and replacement rims and cores with distinct caries texture. In this stage sphalerite consistently replaced galena, and pyrite was consistently replaced by chalcopyrite. The relationship between sphalerite and chalcopyrite is less clear, but in general sphalerite appears to have been the last ore mineral deposited in this stage.

Stage 2 of the paragenesis is divided into three substages (fig. 3). These substages were not considered to be separate main stages because of the following lines of evidence: (1) all three substages were commonly found together in the same fracture; (2) when they occurred in separate fractures there were no distinct crosscutting relationships, and replacement textures among the sulfide minerals were common (indicating at least a slight temporal separation); and (3) the location of the minerals that characterize each substage was consistent within a vein where all three substages occur in the same fracture. Stage 2 is composed of the second and third mineral assemblages described earlier. The substages were distinguished from one another in the field according to the relationships described above (deposition sequence in common fractures, color of quartz, etc.). Microscopic examination revealed that each substage contained characteristic minerals.

Substage A contains mostly quartz. The quartz is clear to white and shows fine banding. Galena, sphalerite, and pyrite are the only sulfides found in this substage. All of the sulfides in this substage are fine grained (<75u) and occur in very small amounts, usually less than 1% of the total substage material. No silver was detected in this substage. The minerals of this substage are always found on the outside of veins at the vein-wallrock contact.

Substage B contains quartz and barite. The quartz is coarse grained (up to 200u in diameter), and is colored various shades of purple. The sulfide minerals in this substage are galena, sphalerite, pyrite, covellite, chalcocite. These sulfides constitute a significant amount, up to 40%, of the material in substage B. Earthy hematite (not specularite) and manganese oxides are also present in this substage in minor amounts. The covellite, chalcocite, and chalcopyrite contain silver in detectable amounts, however no quantitative measurements were made. The minerals of substage B are always found between substage A and substage C material when all three substages occupy the same fracture.

Substage C is composed of coarse grained (up to 2cm in diameter) amethyst, clear quartz, barite, galena, sphalerite, chalcopyrite, pyrite, covellite, chalcocite, bornite, tetrahedrite, undivided sulfosalts, hematite, pyrolusite and other undivided manganese oxides, acanthite,

and native silver. The copper sulfides in this substage do not contain detectable amounts of silver, but the tetrahedrite does. The silver minerals occur late in this substage. These silver minerals are observed in the middle of veins, as linings around vugs, and within vugs. Substage C material always occurs in the middle of the veins where it is found in a fracture with material of substages A and B.

Silver occurs in significant quantities only in substages B and C of the paragenesis. In the discussion of the distribution and zoning of the mineralization in the study area the significance of this temporal characteristic of the silver occurrence will become more clear.

Disseminated Mineralization

This type of mineralization has been studied in the Creede district in detail at the convergence of the Amethyst and OH veins (Giudice, 1980). Very limited exposure of disseminated ore in the mine workings in the southern Amethyst system limits the study of its mineralogy, paragenesis, and distribution somewhat. The mineral assemblage present in the disseminated mineralization in the southern Amethyst system is that of the second assemblage described above. The specific sulfides and the quartz found in the disseminated ore are very similar to those found in substage C of stage 2 of the paragenesis. Silver occurs in the same minerals in both substage C veins and in the disseminated mineralization. Copper sulfides from both are

notably lacking in silver. Clear quartz was found in both substage C vein material and in the disseminated material. No direct crosscutting relationship between disseminated mineralization and vein mineralization was observed.

The disseminated mineralization is very fine grained, rarely greater than 75 μ in diameter. The sulfide particles fill pumice fragments, occur in clear quartz microveinlets in the matrix of healed breccia, and more rarely rim lithic fragments and phenocrysts. Point counts of four samples of disseminated ore indicated that they have up to 3.9% total sulfides. Several replacement textures were observed to show consistent temporal relationships in all polished sections of disseminated ore that were examined. These textures indicated that pyrite was deposited early, and is replaced by covellite, chalcopyrite, sphalerite, chalcocite, and acanthite. Chalcopyrite is replaced by covellite, sphalerite, and acanthite. Bornite is replaced by covellite, and acanthite appeared to be replaced by native silver.

Distribution and Interrelationships of Vein and Disseminated Mineralization

All of the veins that were examined in the study area occur in the Campbell Mountain unit or the Willow Creek unit of the Carpenter Ridge tuff. However, the majority of the vein material studied came from veins in the Campbell Mountain unit. The density of these hanging wall veins

decreases proportionally with distance away from the main Amethyst structures. Veins in the Willow Creek unit are much smaller and much more rare than veins in the Campbell Mountain unit.

Stage 1 veins occur mainly on the lower levels of the mine in the study area, and none were observed above the 450 level (fig. 2). The amount of stage 1 material also decreases to the north. Very little is present as far north as the OH vein.

Stage 2 veins occur from the lowest level of the study area (E level) to above Commodore 2 level (fig. 2). Veins of stage 2 material are present to the south to where the vein horsetails and loses its identity, and at least as far north as Commodore 2 level workings extend. Stage 2 veins containing material of the third mineral assemblage, which is made up primarily of quartz, and iron and manganese oxides, was not observed below Commodore 2 level, except oxides that were considered to be of supergene origin. Manganese carbonates and/or manganese silicates were not observed above C level.

The distribution of disseminated mineralization is not well understood. All of the disseminated mineralization occurs in the Campbell Mountain member of the Carpenter Ridge tuff that forms the hanging wall of the Amethyst fault. It is known, therefore, that the Amethyst fault is the abrupt footwall boundary of disseminated ore, but the

western extent is not exposed in the underground workings or in drill core. The upper or lower extents of this form of mineralization are also not exposed in mine workings or in drill core. Giudice (1980) indicated microfracturing to be a key component of disseminated mineralization. This also appears to be true in the southern one-third of the Amethyst system, for all of the disseminated ore in the study area appears to be confined to zones of dense brecciation which has been healed by clear quartz. Significant quantities of disseminated ore has been observed in drill core that indicate broad vertical and horizontal zones of disseminated mineralization exist within the study area, but the quantity is as yet unknown. Disseminated mineralization does appear to be spatially associated with stage 2 veins, for both of these types of mineralization occur in the greatest quantities where the fracture density in the wallrocks is highest. The details of the nature of this relationship are also unknown. The extent of mine workings and assays from the veins in the lower part of the study area indicate that the ore grade of the veins was not high or consistent. Emmons and Larsen (1913, 1923) and Larsen (1929) describe the veins on Commodore 3 level, which was inaccessible during this study. They indicate that the veins mined from Commodore 3 level contained consistent high ore values, especially high amounts of silver. The extent of the workings in the vicinity of this level, as shown on detailed production maps, is evidence that the area between A level

and Commodore 2 level (fig. 2) is very rich in high grade ore. This area of high grade ore has been noted by Barton et.al. (1977) as the most productive zone in the southern Amethyst system. Data obtained from recently drilled core indicates that the largest amount of disseminated mineralization and high grade vein material occurs between elevations of 3000m and 3200m. Assay data shows that these extensive zones of disseminated ore are remarkably consistent with respect to silver values (fig. 10).

Alteration

It was not the purpose of this study to investigate the alteration in the southern Amethyst vein system, however one important type of alteration was observed. Intense sericitic-illitic alteration caps the ore on the OH vein and is present in much of the rest of the district. This type of alteration was observed only at the northern extent of Commodore 2 level (fig. 2), and therefore its distribution in the study area is believed to be very minor.

Fluid Inclusion Analysis

Many samples of stage 1 vein quartz were examined, but only 4 of these samples were found to contain suitable material for fluid inclusion analysis. Two of these samples from E level were analyzed. Measurements made on 19 primary or pseudo-secondary inclusions indicated homogenization temperatures of 175° to 235°C and salinities of 6.0 to 8.5

equivalent weight percent NaCl. Thirteen primary or pseudo-secondary inclusions found in the other two samples of stage 1 quartz were from D level and these had homogenization temperatures of 178° to 235°C and salinities of 3.8 to 9.6 eq. wt. % NaCl.

Fluid inclusion analysis of stage 2 vein quartz was performed on samples from all three substages. No significant difference was found in either homogenization temperatures or in salinities between the substages on any one level. For example, homogenization temperatures for substage A inclusions on E level averaged 237.5°C and homogenization temperatures for substage B inclusions on E level averaged 238.0°C. Therefore, no distinction has been made between the substages in presenting the results of fluid inclusion analysis of stage 2 material (fig. 4-8).

Fluid inclusion homogenization temperatures show a remarkable relationship with respect to elevation (fig. 4). These temperatures decreased from an average of 238°C on E level to an average of 170°C on Commodore 2 level. This represents a 33% decrease in homogenization temperature over a vertical interval of approx. 315 m. The salinity values averaged 9.1 eq. wt. % NaCl on E level and 6.2 eq. wt. % NaCl on Commodore 2 level, which is also a 33% decrease over the same vertical interval (fig. 5).

Fig. 4. Elevation vs. homogenization temperature (C) for fluid inclusion analysis on stage 2 samples from the accessible mine levels and from four samples of drill core from two elevations. A general trend of increasing temperature with depth is apparent. Elevation of the surface is approx. 3250 m.

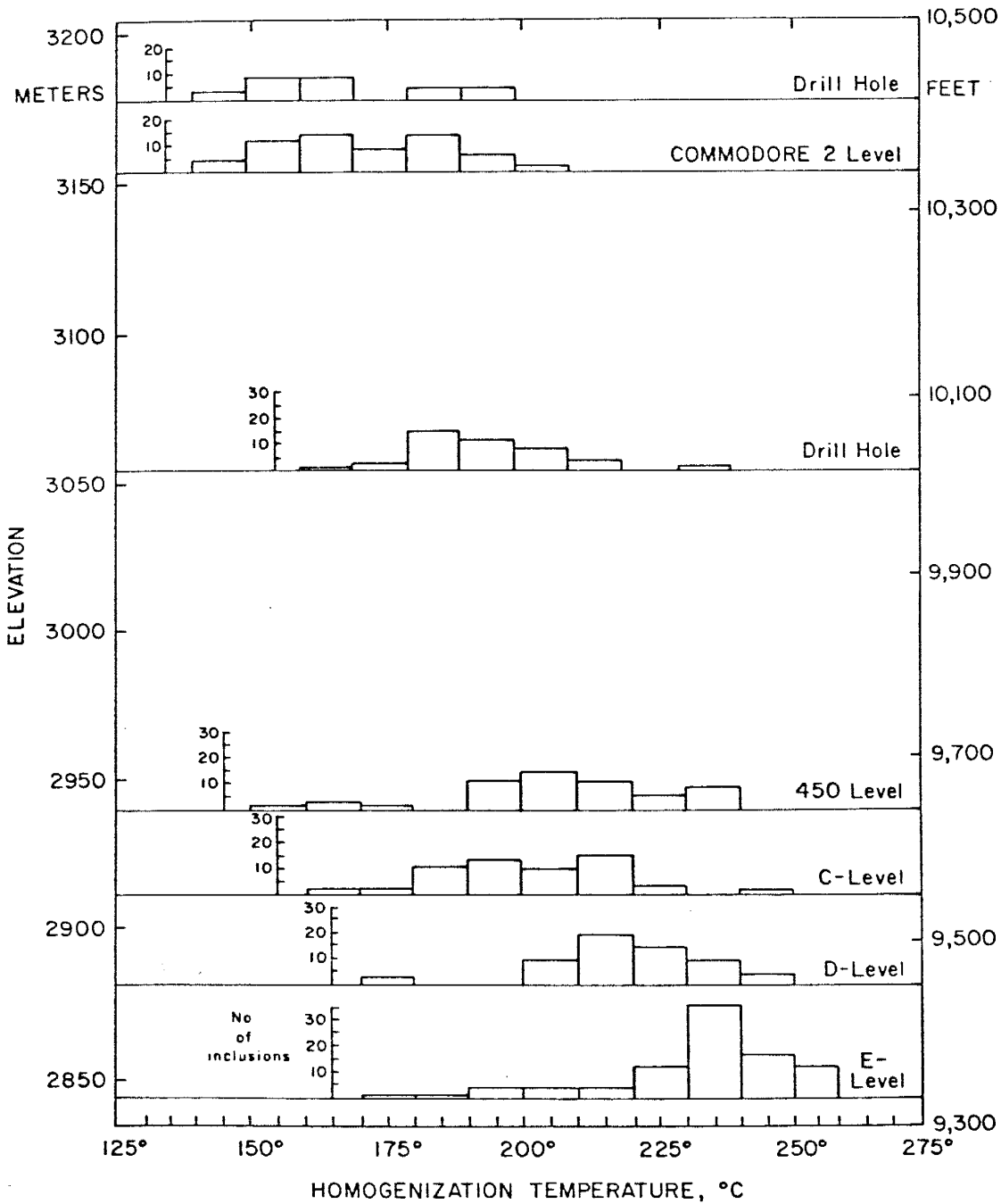
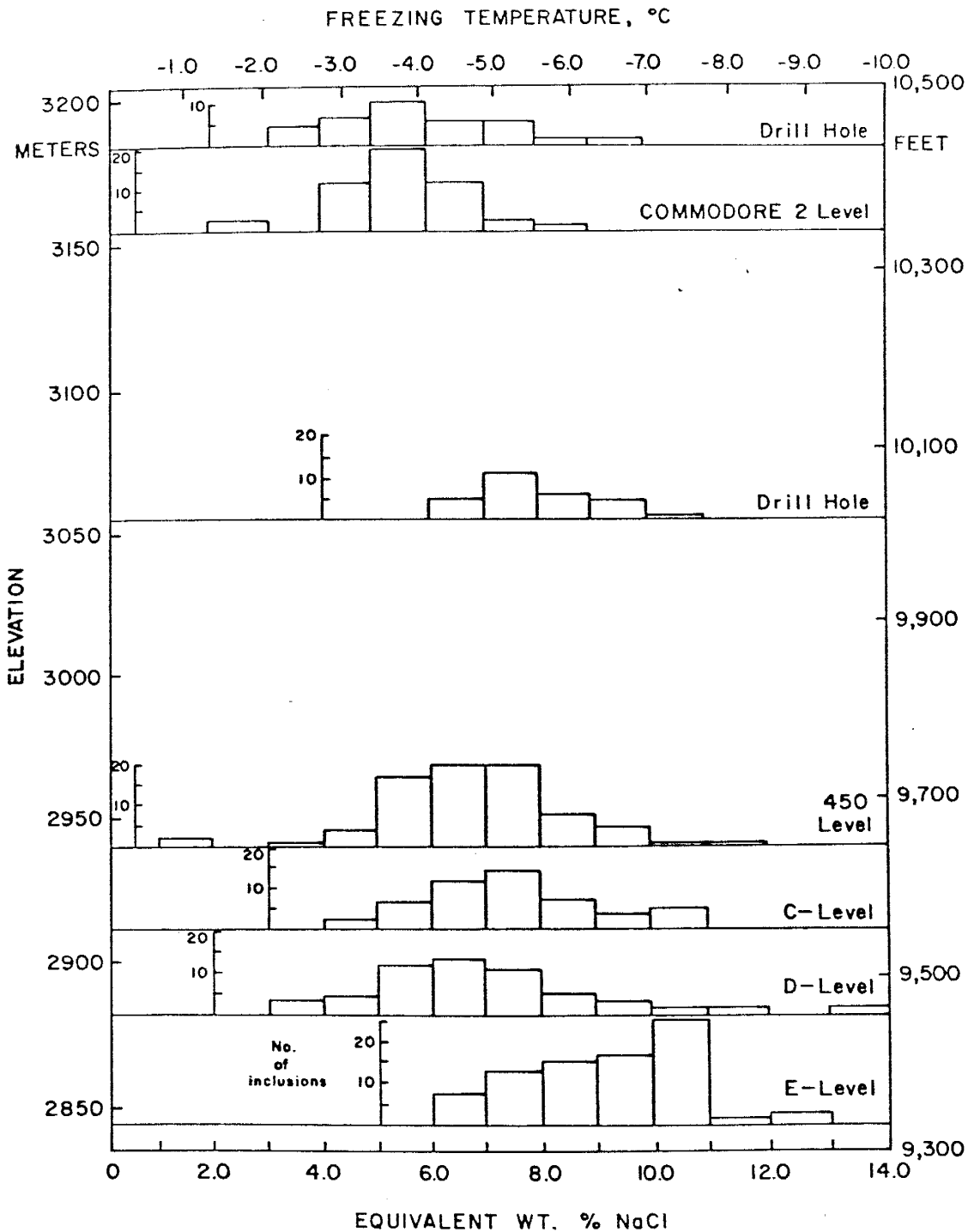


Fig. 5. Elevation vs. equivalent weight % NaCl for fluid inclusion analysis on stage 2 samples from accessible mine levels and from two elevations in drill holes. Though somewhat more irregular than the trend in fig. 4, a general trend of increasing salinity with depth occurs in this data.

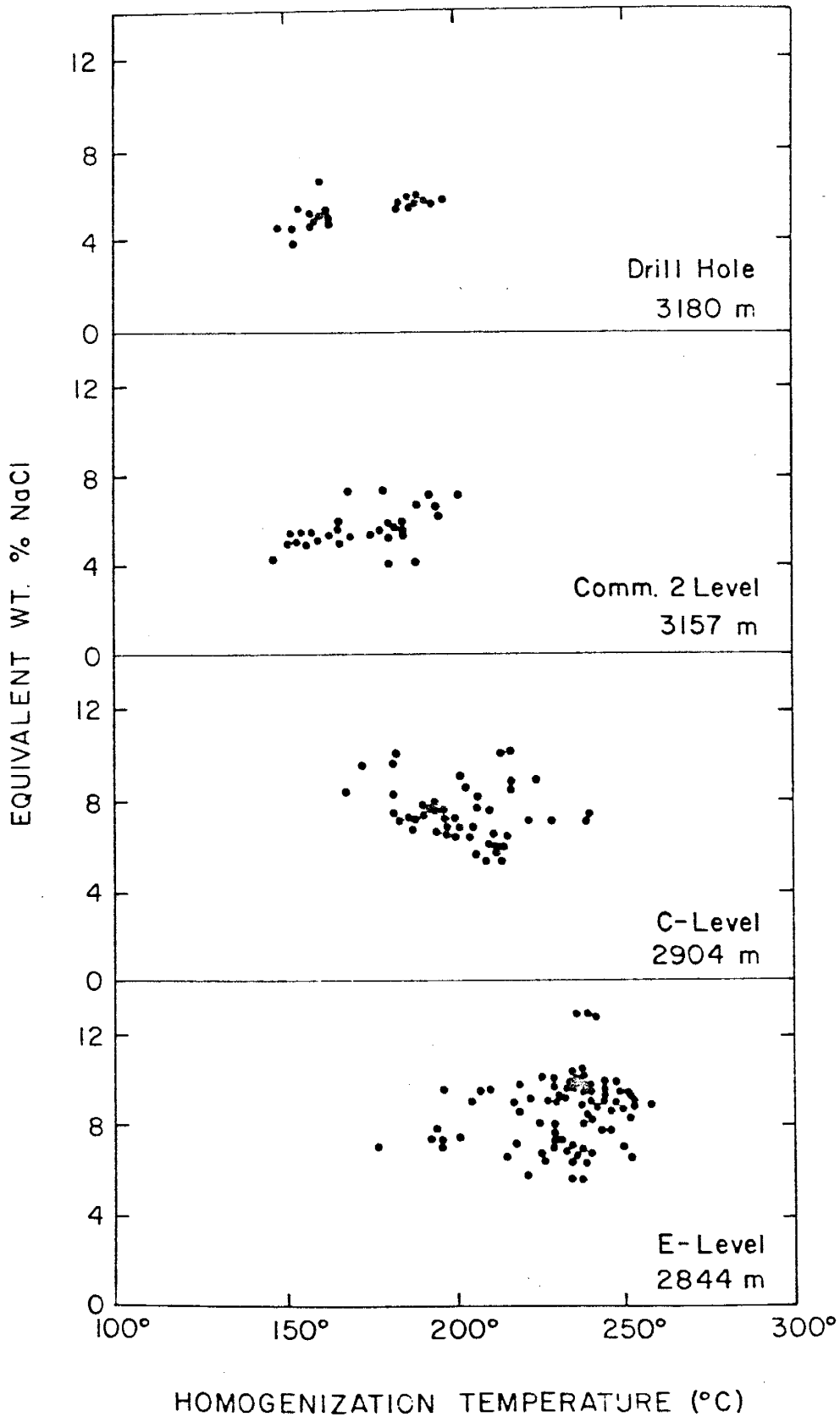


Salinity and homogenization temperature values for individual fluid inclusions also show an interesting relationship with respect to elevation (fig. 6). The inclusions from the lower levels, E and D levels, show very little relationship between salinity and homogenization temperature. However, individual inclusions from Commodore 2 level and from the upper portions of several drill holes show a distinct relationship between salinity and homogenization temperature.

CO₂ and/or CH₄ Rich Inclusions

A total of eight inclusions from samples in the upper portions of several drill holes above Commodore 2 level and from Commodore 2 level (fig. 2) exhibited evidence that indicated they contained high amounts of some type of gas. The small vapor bubble present in two of these inclusions disappeared when the inclusions froze at temperatures between -33°C and -40°C . This solid ice material melted at temperatures that were similar to the melting temperatures found in many of the inclusions that were analyzed (-2.5° to -5.0°C). However another object that did not resemble a vapor bubble remained as the inclusions were slowly heated above the melting temperatures of the ice. At temperatures that varied for each of these inclusions from 0.0°C to $+7.8^{\circ}\text{C}$ this unidentified "bubble" instantaneously changed from a large irregular shape with low relief to a vapor bubble of normal appearance with characteristically high

Fig. 6. Equivalent wt. % NaCl vs. homogenization temperature for individual fluid inclusions in stage 2 samples from three representative levels and from samples in drill core. C-level and E-level data shows no relationship between these two properties. Data from Commodore 2 level and from the drill core above this level do show a somewhat consistent relationship between salinity and homogenization temperature.



relief. Similar behavior of fluid inclusions has been reported by Roedder (1967). This behavior is caused by metastable ice present in these inclusions, (Roedder, 1967). Six other inclusions contained both ice and very small vapor bubbles at temperatures $<-10^{\circ}\text{C}$. As these inclusions were slowly heated the size of the vapor bubble increased as the ice melted and became smaller. Complete melting of the ice usually did not occur until the temperature was raised above 0.0°C . Collins (1979) concluded that this behavior indicates that these inclusions contain high amounts of CO_2 and/or CH_4 as clathrate compounds. It is not possible to determine which of these gases, CO_2 or CH_4 , is present in the inclusions without actual analysis of the gases in the inclusions, and no such analysis were performed in this study. Therefore the only interpretation possible is that these inclusions contain high amounts of one or both of these two gases.

No evidence of boiling was found in any of the fluid inclusions from the study area other than this presence of high amounts of CO_2 and/or CH_4 in a limited number of inclusions.

Discussion

Mineralogy and Paragenesis

The mineralogy and paragenesis of the Creede ores have been described in several recent reports (Giudice, 1980; Bethke and Rye, 1979; Wetlaufer, 1977; Barton et.al., 1977; Roedder, 1960, 1974; Bethke and Barton, 1971; and Steven and Ratte, 1965; Bethke et.al., 1960). The study of the complete time-space relationships, however, is not yet complete. Comparison of the mineralogy and paragenesis of the southern Amethyst vein system with that of the entire district, fig. 7, (Bethke and Rye, 1979) indicates that all of the mineralization in the study area occurred early in the mineralizing event. "A" stage mineralization defined by Bethke and Rye, (1979), consists of quartz and rhodochrosite, which is also present in the stage 1 assemblage of this study, (fig. 3). Stage B in fig. 7 is probably the same as stage 2 described in the current study in fig. 3. "B" stage, in both fig. 7 and fig. 3, is the stage in which most of the silver occurs. The minerals found in stages C, D, and E in the summary of the paragenesis of the Creede ores (fig. 7) appear to be absent, with the exception of minor marcasite, from the southern Amethyst vein system. Evidence for the absence of C, D, and E stages in the study area is: (1) all sulfides in the study area are fine grained, whereas stage D is described as being very coarse grained; (2) no fluorite or

Fig. 7. Summary of the paragenesis of Creede ores,
after Bethke and Rye (1979).

Stage	Characteristics	Distribution
E stage (youngest)	Fibrous pyrite with some marcasite and stibnite; generally high in orebodies and commonly on cross-cutting fractures	District-wide
D stage	Relatively coarse-grained sphalerite, galena, chalcopyrite, and quartz, some hematite; silver minerals notably absent; probably stage of illite alteration; subdivided into three substages on basis of color banding in sphalerite: inner light, middle dark, and outer light	Northern parts of OH, P, and Amethyst veins; poorly developed on Bulldog Mtn. vein system as developed thus far
C stage	Volumetrically minor, sits on deep etch of earlier B stage; fluorite overgrowing siderite-manganosiderite and quartz; most fluorite deeply etched—commonly completely removed	Recognized only in northern parts of OH, P and Amethyst veins thus far
B stage	On OH, P, and northern Amethyst veins, relatively fine grained sphalerite, galena, chalcopyrite, chlorite, hematite, pyrite, and with some tetrahedrite-tennantite; on southern Amethyst vein and on Bulldog Mtn., the vein system consists of banded barite-sulfide with quartz; sulfides, mainly sphalerite and galena with much tetrahedrite-tennantite and other sulfo-salts; native silver common	District-wide
A stage (oldest)	Primarily quartz with minor chlorite and sulfide on OH and P veins and on northern $\frac{2}{3}$ of Amethyst vein; on southern part of Amethyst vein and on the Bulldog Mtn. vein system, A stage consists mainly of both quartz and rhodochrosite	District-wide

siderite, the assemblage described in stage C, was found in the study area; and (3) only one small (2cm wide) vein of marcasite was found in the northern-most workings of Commodore 4 level within the study area (fig. 2).

Decrease of Homogenization Temperatures

Many fluid inclusions studies that have been reported indicate that no significant temperature or salinity trends have been related to elevation (Rye and Sawkins, 1974; Norman, 1976; Barton et.al., 1977; Kelly and Rye, 1979). The fluid inclusion homogenization and salinity data in this study area (fig. 4) represent an unusual occurrence. The data shows a decrease in homogenization temperature of approximately 60 C in a vertical interval of about 330m. This represents a geothermal temperature gradient of approx. 180°C/km, which is well above the gradient of 30° to 35°C/km for average areas (Norton and Cathles, 1979). In several active geothermal areas, however, the geothermal gradient is reported to be well over 100 C/km (Ellis, 1979; Weissberg et.al., 1979).

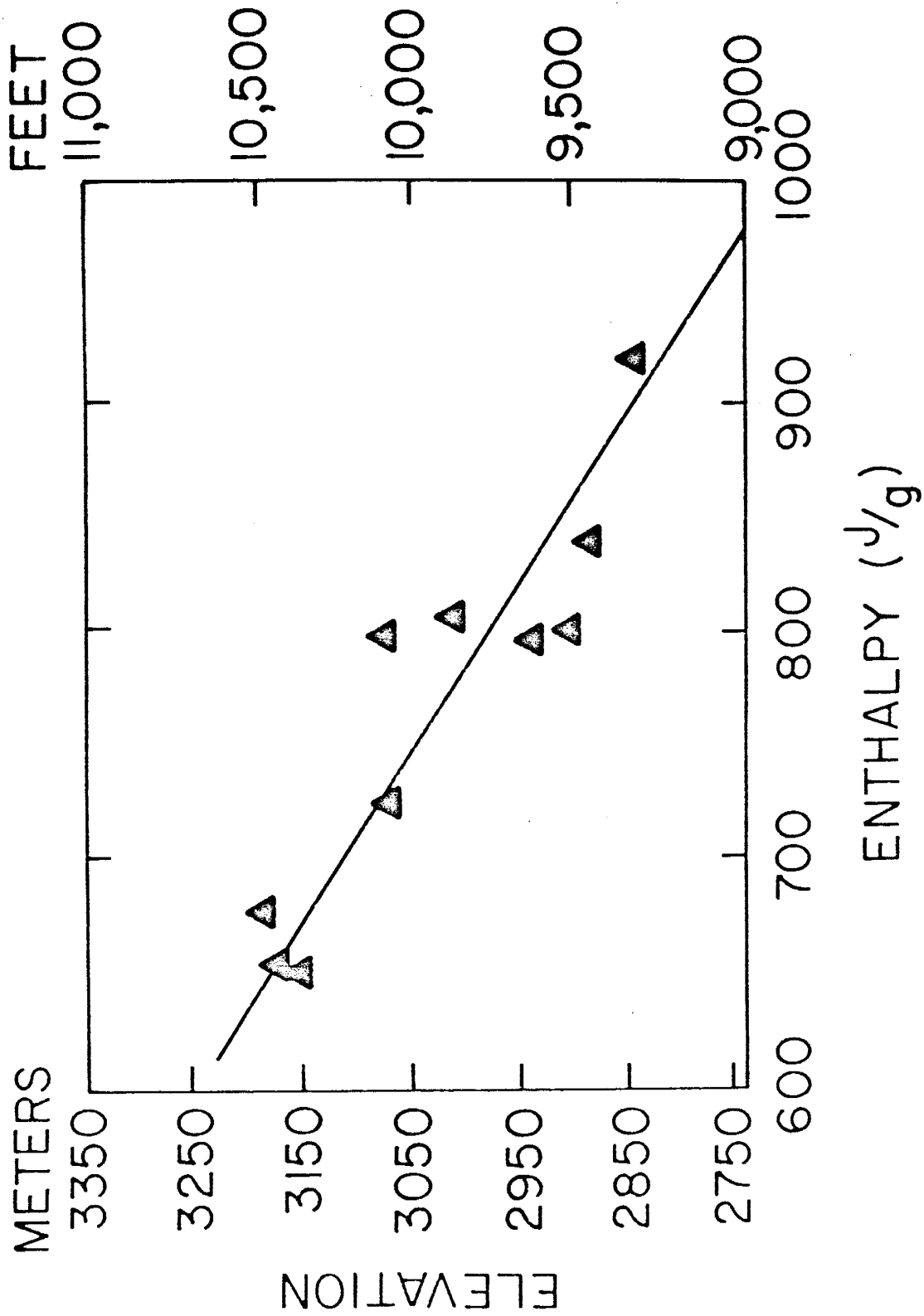
It is apparent that the ore fluids in the study area were cooling vertically at a very rapid rate. This cooling was due to either conductive or convective cooling processes. In order for conductive processes to cool the ore fluids at the measured vertical gradient the vertical fluid flow rate would have to be unreasonably slow (Truesdell et.al., 1977; Barton et.al., 1977). Conductive

heat loss would not explain the corresponding decrease in salinity over the same vertical interval (fig. 5), or the relationship between salinity and homogenization temperature in individual inclusions with respect to elevation (fig. 6). It has been shown in active geothermal areas that where high geothermal temperature gradients exist they are due to convective heat loss, which is often caused by mixing of the deeper hot solutions with shallow cooler solutions (Ellis, 1979; Weissberg et.al., 1979; Truesdell and Fournier, 1976).

Enthalpy of Fluids

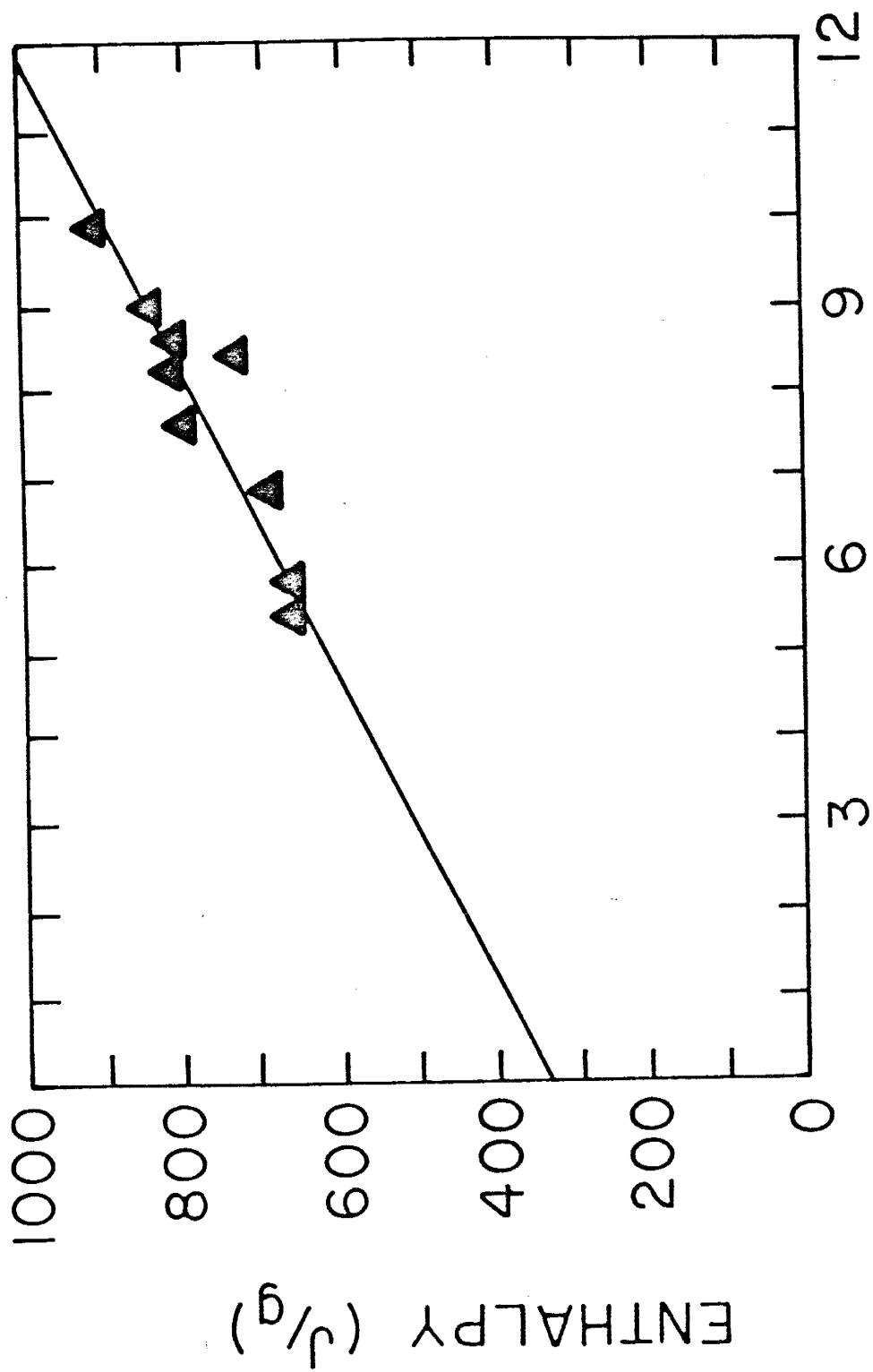
The enthalpy of fluids in geothermal systems is often used in literature concerning geothermal areas to represent the heat "content" of the fluids in a more accurate way than is possible by the use of just temperature. Fournier (1979) uses enthalpy-chloride diagrams to estimate both temperatures possible at depth and temperatures possible near the surface in a geothermal system. Enthalpy-chloride diagrams are also used to determine the degree of mixing of fluids in geothermal environments (Fournier, 1979; Truesdell and Fournier, 1976; Fournier and Truesdell, 1974). The enthalpy of the fluid in fluid inclusions in the study area were calculated according to data in Haas (1976) and Haas and Potter (1977). The enthalpy of these fluids shows a distinct relationship with elevation (fig. 8). This linear decrease in enthalpy with elevation is

Fig. 8. Elevation vs. enthalpy for fluid inclusions in stage 2 samples from 10 different levels. The enthalpy values were calculated from information in Haas (1976) and Haas and Potter (1977). The line through the data points was calculated by linear regression analysis and has an R square value of 0.840. Values used to calculate the enthalpies are average values for the fluid inclusions on each of the levels represented.



consistent with a system in which ore fluids mix with increasing amounts of cooler and more dilute fluids near the surface. Characteristics of a fluid with which the ore solutions may have been mixing are estimated by making use of the linear relationship between enthalpy and salinity of the fluid inclusion data (fig. 9), (Truesdell and Fournier, 1976; Fournier, 1979). At 0 eq. wt. % NaCl the enthalpy of a fluid along this line is 327 J/g (joules/gram), which corresponds to temperature of 78°C. Although this temperature is above that of normal groundwater, it is well within the range of temperatures of waters found in the upper portions of stacked geothermal convections systems (Sigvaldson and Cuellar, 1971; Arangano et.al., 1971; Noguchi et.al., 1971; Nakamura et.al., 1971; Ellis, 1969; Ellis and Mahon, 1977; Elders, 1965; Fournier, 1979; Grose, 1979; Fournier and Truesdell, 1974; Truesdell and Fournier, 1976). Wetlaufer et.al. (1978) examined the Creede district as a fossil geothermal system. They suggested the possibility that a shallow circulating system may have existed over the more deeply circulating system during mineralization. The data presented in this study support their suggestions that Creede may be a fossil geothermal system.

Fig. 9. Plot of enthalpy vs. salinity for the same 10 levels shown in fig. 8. The salinities are average salinities for all of the fluid inclusions from the stage 2 samples analyzed on each level. Predictions according to Fournier (1979) as to the nature of waters in the postulated dilute shallow circulating cell are possible by extending the linear regression line toward conditions of lower salinity and corresponding enthalpy values. At 0 eq. wt. % NaCl the enthalpy = 327 J/g, which is equal to a temperature of approx. 78°C.



EQUIVALENT WT. % NaCl

Chemical Controls on the Properties of Mineralization

Barton et.al. (1977) suggested that ore deposition was due to cooling of the ore fluids and to a slight rise in pH due to boiling. They also determined that the metals were most likely transported as chloride complexes. Metals have been found in solutions as chloride complexes in several geothermal systems (Ellis, 1969; Shanks and Bischoff, 1977; Skinner et.al., 1967). It has been determined that metals may be transported in solution as chloride, sulfide, sulfate, fluoride, ammonia, and as organic complexes, with the first three as by far the most common. The concentration of sulfur species in solutions from fluid inclusions from the OH vein at Creede was found to be 0.02 molal, compared to 1.0 molal for chloride species in solution (Barton et.al., 1977). The high amount of chloride in solution relative to sulfur seems to justify the assumption of metal-chloride complexes as the dominant form of metal transport.

The following mechanisms may cause precipitation of metal-chloride complexes from solution: (1) increased concentration of sulfur in solution; (2) increase in pH; (3) decrease in chloride concentration; (4) decrease in temperature; and (5) reducing oxygen fugacity (Barnes, 1979; Barnes and Czmanske, 1967). The widespread occurrence of intense sericitic alteration and direct fluid inclusion evidence indicates that boiling occurred widely at

Creede during mineralization (Barton et.al., 1977). Little evidence of boiling was found in the fluid inclusions from the southern Amethyst system, nor was the occurrence of intense sericitic alteration widespread in the study area. Therefore a rise in pH of the fluids due to boiling is rejected as an important factor controlling the distribution of ore material in the study area.

Fluid inclusion data (figs. 4-8) indicate that a significant amount of cooling and dilution of the ore fluids occurred in the study area during the mineralizing event. This is most easily explained by mixing of the laterally flowing ore fluids with cooler dilute fluids near the surface (fig. 10). This rapid cooling and dilution (decreasing the chloride concentration) would have resulted in precipitation of the ore and gangue minerals from the ore solutions. The broad lateral and vertical zones of disseminated mineralization of consistent silver content present at shallow depths (50m to 200m below the surface) in the study area also suggest that precipitation due to mixing solutions may be an important control in the distribution of ore grade material. The proposed zone of mixing also corresponds with the area of the most productive zone on the Amethyst vein (fig. 10) described by Barton et.al. (1977), Emmons and Larsen (1913, 1923), and Larsen (1929). The fine grained nature of the mineralization in the study area is evidence that deposition was probably rapid, which might be expected in a mixing environment.

Surface Reconstruction

The fluid inclusions from the study area did not contain positive evidence that the fluids had boiled. Evidence of high amounts of CO_2 and/or CH_4 in some of the inclusions from the upper levels of the study area, and limited amounts of intense sericitic alteration are taken as indirect evidence that boiling may have occurred locally. The samples from the study area that contain this possible evidence of boiling show homogenization temperatures that average 170°C . Boiling curve data (Haas, 1971) show that these samples were under 80-100m of water in order to restrain boiling to these temperatures. Isolated occurrences of sericitic alteration "cap", located near the samples that contain the high CO_2 - CH_4 inclusions, are at elevations that are above the sericitic alteration zone that overlies the OH orebody. This indicates that this sericite "cap" slopes up to the south (fig. 10). Therefore the Miocene surface over the hydrothermal system would have had to slope down to the south for the correct hydrostatic pressure to be maintained to restrain boiling (at the temperatures that have been measured) in both the OH vein and the southern Amethyst system simultaneously.

Summary and Conclusions


Characteristics of Mineralization

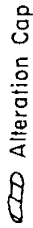
Mineralization in the southern one-third of the Amethyst vein system is unlike the mineralization that has been described in much of the Creede district. Vein material was deposited in open spaces that resulted from normal faulting. These veins occur in the Campbell Mountain member of the Carpenter Ridge tuff, which forms the hanging wall of the Amethyst fault. Fracture density, and associated vein density, decrease away from the main Amethyst structure. Zones of intense fracturing and brecciation appear to be associated with variations in the dip and strike of the main fault structure. Broad zones of disseminated mineralization occur in these zones of brecciation in the hanging wall of the fault, but the relationship of this disseminated ore to the vein mineralization is not known. The amount of disseminated mineralization is also not known.

The paragenesis is divided into two main stages. Stage 1 is characterized by rhodochrosite, clear to white quartz, minor amounts of base-metal sulfides, and a lack of silver. Stage 1 veins occur for the most part on the lower levels of the mine. Stage 2 is a complex stage made up of three substages. Although the temporal relationship of these substages has been established, the limited amount of time separating them, their very close spatial relationship, and

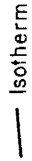
Fig. 10. Modification of the model proposed by Barton et.al. (1977) with shallow circulating system added near the southern end of the Amethyst vein system according to the interpretation of the results of fluid inclusion and mineralogical analysis of this study. Most productive zone on the Amethyst vein system inferred from field observations, examination of mine production records and maps, recently drilled core samples, and from early reports by Emmons and Larsen (1913, 1923) and Larsen (1929). Alteration "cap" extends to the north but is not shown.

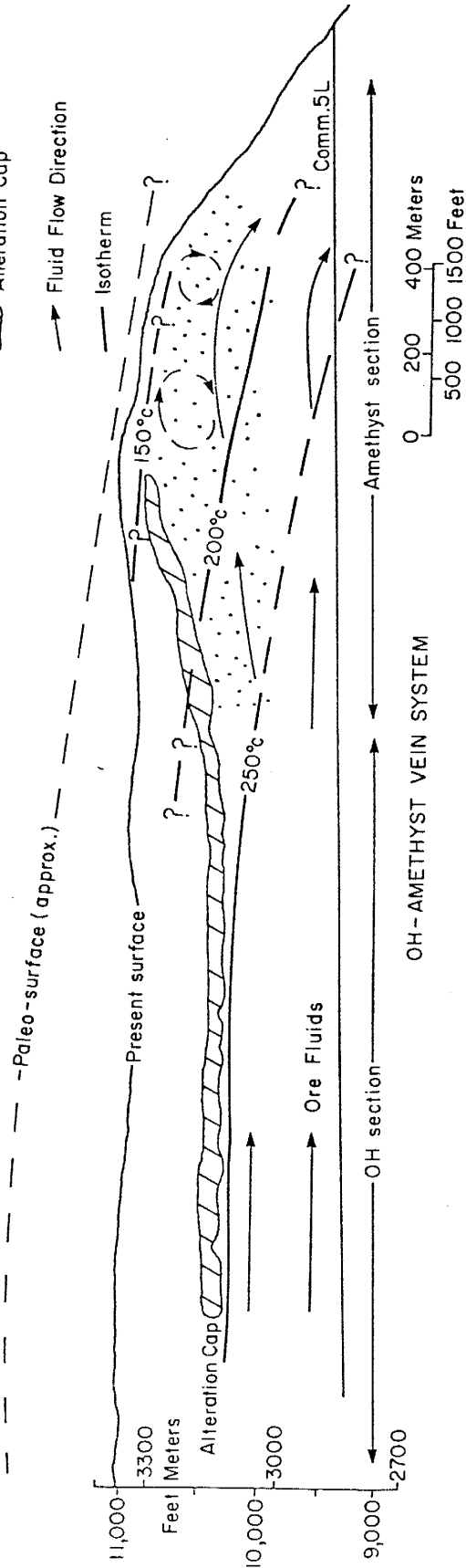
EXPLANATION

 Most Productive Zone

 Alteration Cap

 Fluid Flow Direction

 Isotherm



the similarity of the fluid inclusion data from quartz from each substage suggest that all three substages represent one complex event. Substage A is composed of clear to white quartz with minor amounts of base-metal sulfides. No silver was detected in this substage. Substage B contains amethyst and barite, abundant base-metal sulfides, and small amounts of iron and manganese oxides. The copper sulfides in this substage contain significant amounts of silver. Substage C contains clear quartz and amethyst, base and precious metal sulfides, sulfosalts, iron and manganese oxides, and native silver. The silver in this substage did not occur in the copper sulfides.

The disseminated mineralization appears to be related to Substage C on the basis of similar mineralogy, but no direct genetic evidence for this assumption was observed. Drill hole data and limited underground exposure of disseminated ore indicate that this type of mineralization occurs in broad densely fractured zones that have been healed by clear quartz and contains up to 3.9% total sulfides. These zones of disseminated ore occur between elevations of 3000m and 3200m.

Fluid inclusion measurements were made mostly on stage 2 vein-quartz material, due to the lack of suitable material that was found in stage 1 quartz. Stage 2 inclusions from the lower levels of the mine had average homogenization temperatures of 238°C and average salinities of 9.5 eq. wt.

% NaCl. Analysis of inclusions from the top levels of the mine had average homogenization temperatures of 170°C and average salinities of 6.5 eq. wt. % NaCl. Inclusions from intermediate levels of the mine showed values consistent with the linear trend of homogenization temperatures and salinities from the upper and lower levels of the mine. Enthalpy values calculated from fluid inclusion data obtained in this study show linear relationships when plotted against both salinity and elevation. These linear relationships are interpreted to indicate that mixing of hot (hydrothermal) waters and cooler (shallow) waters occurred during mineralization. Hydrothermal fluids flowing laterally along the top of a freely convecting cell encountered cooler dilute waters in the southern portion of the Amethyst system. These two fluids mixed, with the degree of mixing decreasing with depth. Mixing caused rapid dilution and cooling of the ore fluids which resulted in rapid deposition of metals from solution.

Application to Proposed Hydrothermal Models

The location of the mineralization in the southern one-third of the Amethyst vein system in the Creede district supports the idea that the hydrothermal ore solutions flowed laterally from north to south. Isothermal lines, interpreted from fluid inclusion data from the OH vein and from the southern Amethyst system, slope down to the south (fig. 10). This also suggests that the ore solutions

entered the study area from the north. The slope of these isotherms also indicates that the ore fluids were probably descending or cooling rapidly with increasing elevation. The fluid inclusion data and the distribution of the broad zones of disseminated mineralization (fig. 10) suggest that perhaps the hydrothermal ore fluids were mixing with a shallow circulating system of dilute cooler waters. The presence of such a shallow system, though not a major component in the proposed hydrothermal model (Steven and Eaton, 1975; Barton et.al., 1977; Behtke and Rye, 1979), has been proposed previously for the Creede district (Wetlaufer et.al., 1978). A mixing model also helps to explain possible controls on precipitation in the absence of boiling. Since little evidence was found to indicate that significant amounts of boiling occurred in the study area, in contrast to large amounts of boiling that occurred on the OH vein, mixing of hydrothermal solutions with cool dilute solutions provides a mechanism for rapid precipitation of ore material from southward flowing and descending solutions.

Future Research

Although the mixing model proposed in the preceding discussion is not a new idea, the criteria for the recognition of mixing environments in fossil geothermal systems is not well documented. Clearly more work is needed concerning this subject. Detailed stable isotope studies of the southern portion of the Creede district may help to determine if mixing actually did occur. Further fluid inclusion and mineralogic studies with more complete sample distribution in the "unstudied" area between the southern Amethyst vein and the OH vein are also needed to define why the characteristics of the mineralization in these two areas, that are part of a connected vein system and are located only 2km from one another, seem to be so different. Studies of the mineralization in the Creede Formation are also needed for a better understanding of the complexities of the southern portion of the Creede district.

APPENDIX A

Fluid Inclusion Data and Sample Locations

The distribution of samples on the lower levels of the mine is very good due to excellent exposure. In fig. 11 the distribution of samples on E-level is shown by the green symbols. The geology on E level is typical of the geology on all of the levels that were mapped during this study. Detailed mapping and sampling was performed on E, D, C, Commodore 4, 450, and Commodore 2 levels, (fig. 12). Levels between 450 level and Commodore 2 level were inaccessible during the study.

Fig. 11. Generalized cross section looking north through the Archimedes Raise area. Samples were taken from E, D, C, Commodore 4, drill core from between the 450 level and Commodore 2 level, from Commodore 2 level, and from drill core above Commodore 2 level. The dashed workings are projected onto the section from in front of the section and dotted workings are projected onto the section from behind the section. The geology is generalized with members of the Carpenter Ridge Tuff represented as: Tbc, Campbell Mountain member; and Tbw, Willow Creek member. The Creede Formation is shown as Tc.

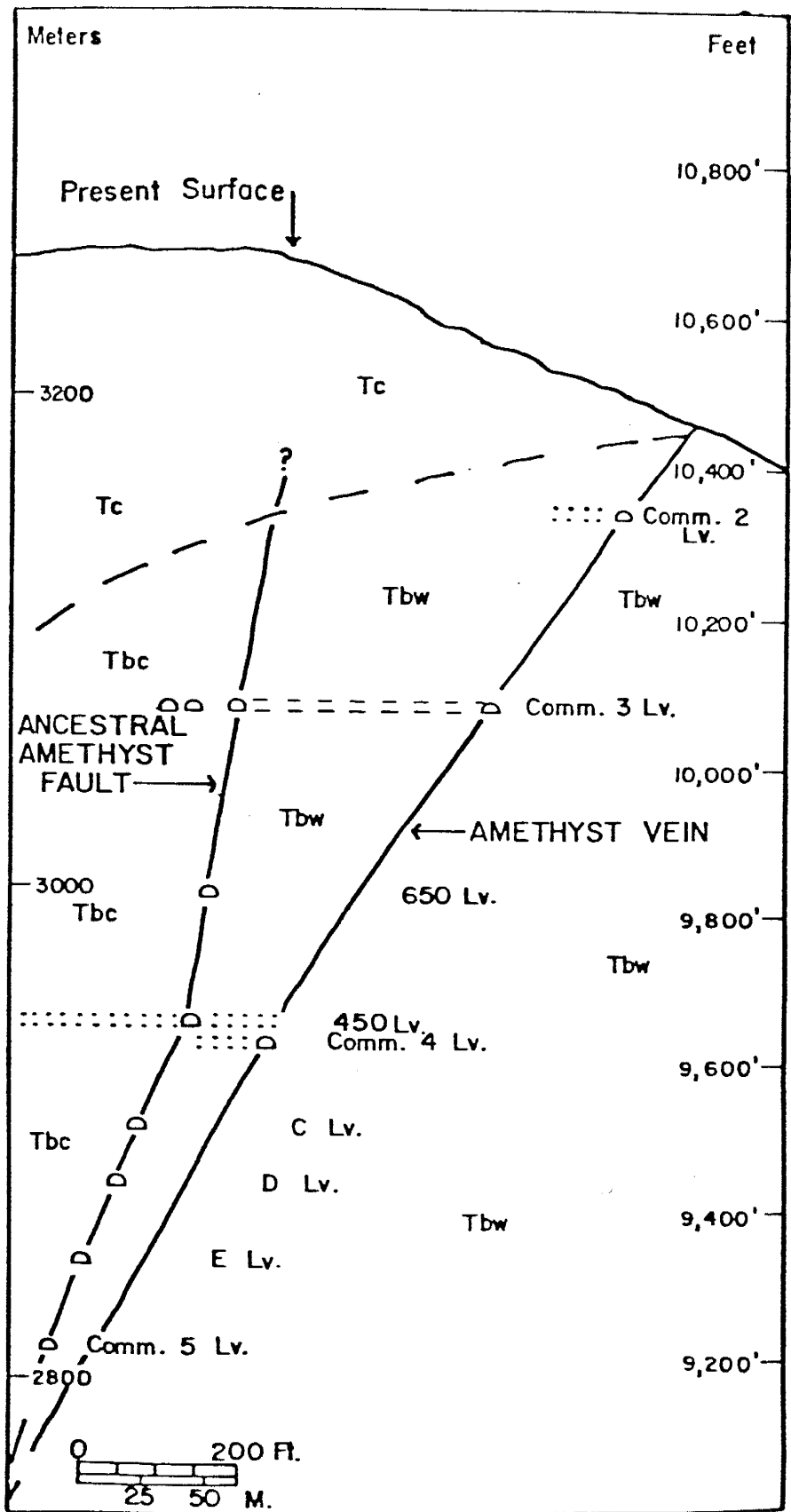
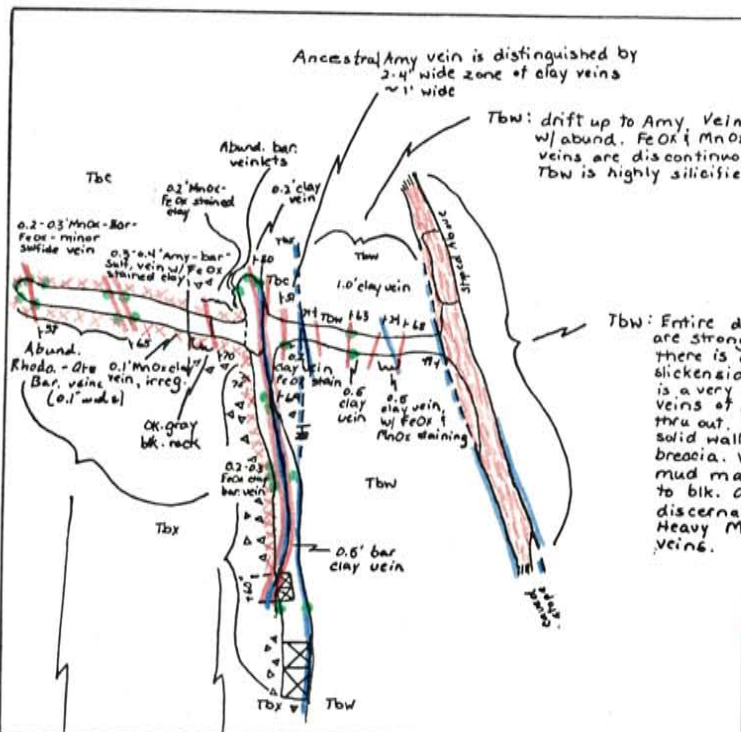


Fig. 12. Geologic map of E-level, considered to be typical of the geology of the workings in the study area. Structures less than 6" wide were generally not shown. The west cross cut on this level contained abundant relatively flat lying veins of stage 1 material, but these were mostly 2" to 3" wide, and thus do not appear on the map. Many samples taken from this level are shown as green symbols, even though the structures that they represent may not appear on the map.



Tbw: drift up to Amy Vein is extremely brecciated w/ abund. FeOx + MnOx staining along fract. veins are discontinuous because of brecciation. Tbw is highly silicified. Veins are clay.

Tbw: Entire drift is on Amy Vein. All fract. are strongly silicified Tbw. On east wall there is a face of solid Tbw - but no slickensides present. Zone within drift is a very intense mud breccia w/ irreg. veins of Amy-sulfides - bar - running thru out. West wall of drift is not a solid wall but is also intense mud breccia. Variable frag. of Tbw w/ in mud matrix. Mud is from brn-yel brn to blk. Original texture of Tbw not discernable due to intensity of silicification. Heavy MnOx staining on most of irreg. veins.

ETB: early tectonic breccia
 Fault
 Intense fracturing = high density of small veins
 Vein
 Sample location

Tbc: Most of section is bleached w/ small parts being dk red - blk + very silicified. The southern 60' are very brecciated w/ Tbw frag. common. Barite veinlets are also abund. in this area. striking N-S. Frac. in this area tend to strike N-S. Sulfides were found in Tbc wallrock. Abund. FeOx + MnOx along fract. w/ minor amt. of grn. clays. South 60' had abund. clay along east wall suggesting fault may be close.

Tbc: shows high degree of variability. Near drift on E-end Tbc appears dk gray-blk color w/ abund. pumice and lithic frag. w/ very irreg. alignment. Very abund. small veinlets of prob. silica + sulfides cut some frag. and are sympathetic around others. Toward west the rocks show a grad. change to a lighter med. red color. Compactional alignment is readily apparent to west although abund. clay + silica veinlets (up to 2cm) continue to cut thru wallrocks). Most of the Tbc w/ in main drift (in middle of x-cut) shows very strong bleaching + this is also seen locally, strong but irreg. thru out x-cut (esp. near larger veins) FeOx + MnOx clays coat most of the mod. amts. of fract.

Tbc: next to Amy fault is highly silicified and bleached. Tbc is brecciated near the fault + rocks not brecciated have good relief texture. Matrix of the breccia has diasem. Sulfides Abund. MnOx - FeOx staining on fract. no Ca staining present.

N
↑

E Level

1" = 40'

Table 1. Fluid inclusion data and general sample locations. All of these inclusions were measured in quartz. Abbreviations: "*" indicates samples from stage 1; "***" indicates samples from substage A of stage 2; "****" indicates samples from substage B of stage 2; "*****" indicates samples from substage C of stage 2. Inclusion type abbreviations; 1 are primary inclusions; p2 are pseudo-secondary inclusions; 2 are secondary inclusions; "Clath." are inclusions containing CO₂ and/or CH₄ clathrate compounds.

Table 1. Fluid Inclusion Data

Sample number	Location	Incls. type	Filling temperature (°C)			Salinity (equiv. wt. % NaCl)		
			No. Incls.	Temp. range	Mean temp.	No. incls.	Saln. range	Mean Saln.
AR1-E**	East rib,	1 ^o	6	229 ^o -241 ^o	237 ^o	6	5.8-12.8	10.6
	E-Lv. drift	p2 ^o	5	225 ^o -238 ^o	232 ^o	4	6.9-7.2	7.0
	near chute	2 ^o	8	226 ^o -247 ^o	234 ^o	7	8.0-10.6	10.2
AR2-E****	West rib,	1 ^o	23	222 ^o -253 ^o	236 ^o	20	5.9-10.8	9.9
	E-Lv. drift	p2 ^o	6	231 ^o -240 ^o	236 ^o	3	9.5-10.1	9.8
	near chute	2 ^o	4	203 ^o -230 ^o	220 ^o	2	10.0-10.6	10.2
AR4-E****	West rib,	1 ^o	5	235 ^o -238 ^o	237 ^o	5	10.0-10.9	10.7
	E-Lv. drift	p2 ^o	3	219 ^o -238 ^o	232 ^o	4	10.6-11.0	10.8
	near chute	2 ^o	4	228 ^o -234 ^o	231 ^o	4	9.9-10.1	10.0
AR11-E***	South rib, E-	1 ^o	9	237 ^o -258 ^o	246 ^o	9	9.0-10.1	9.6
	Lv west x-cut near face							
AR13-E***	North rib, E-	1 ^o	8	229 ^o -253 ^o	236 ^o	8	7.6-9.5	8.2
	Lv west x-cut	p2 ^o	3	232 ^o -240 ^o	235 ^o	3	8.0-8.4	8.1
	near face	2 ^o	4	225 ^o -230 ^o	228 ^o	4	7.9-8.1	8.0
AR12-E*	North rib, E-	p2 ^o	7	218 ^o -235 ^o	222 ^o	7	6.0-7.2	6.7
	Lv west x-cut near face							
AR15-E**	South rib, E-	1 ^o	7	240 ^o -251 ^o	247 ^o	7	8.0-8.8	8.5
	Lv west x-cut							
AR16-E*	South rib, E-	1 ^o	12	175 ^o -217 ^o	200 ^o	12	7.0-8.5	8.0
	Lv west x-cut 30' fr. face							
AR19-E***	Face of	1 ^o	8	221 ^o -240 ^o	233 ^o	-	-	-
	E-Lv drift							
AR20-E**	Face of	1 ^o	6	204 ^o -252 ^o	234 ^o	7	7.8-8.1	8.0
	E-Lv drift							
AR24-E****	West rib,	1 ^o	9	221 ^o -258 ^o	235 ^o	8	7.9-9.4	9.0
	E-Lv drift							
	S.of chute							

Table 1 (continued)

Sample number	Location	Incls. type	Filling temperature (°C)			Salinity (equiv. wt. % NaCl)		
			No. Incls.	Temp. range	Mean temp.	No. Incls.	Saln. range	Mean saln.
AR5-D**	West x-cut, D-Lv. 1st vein W. of drift	1 ^o	10	137°-253°	220°	10	6.9-12.4	9.6
AR10-D***	West x-cut, D-Lv. 2nd vein W. of drift	1 ^o p2 ^o	6 27	228°-234° 200°-232°	232° 220°	6 25	7.7-8.0 6.0-7.8	7.8 7.6
AR11-D*	West x-cut, D-Lv. 25' W. of drift	1 ^o 2 ^o	7 6	178°-210° 207°-225°	198° 215°	7 6	3.8-9.6 5.5-6.1	6.8 6.0
AR13-D*	West x-cut, D-Lv. 40' W. of drift	1 ^o	6	204°-234°	219°	6	6.4-6.6	6.5
AR14-D**	West x-cut, D-Lv. Same vein as above	1 ^o	8	177°-255°	230°	8	7.2-9.4	8.1
AR1-C****	South rib, C-Lv. x-cut	1 ^o p2 ^o	4 4	168°-217° 182°-216°	187° 199°	4 4	8.4-9.6 10.1-10.4	9.2 10.2
AR2-C***	North rib, C-Lv. x-cut	1 ^o p2 ^o 2 ^o	4 10 11	181°-207° 212°-241° 184°-201°	198° 225° 192°	5 6 6	8.2-8.8 7.0-9.0 4.0-6.4	8.5 7.8 6.1
AR3-C**	Face of C-Lv. drift	1 ^o p2 ^o	4 9	187°-205° 183°-200°	198° 192°	4 8	6.4-7.0 5.6-7.7	6.8 7.2
AR4-C****	Face of C-Lv. drift	1 ^o p2 ^o	7 8	190°-214° 198°-214°	201° 209°	7 9	5.6-7.9 5.6-7.5	7.3 7.1
AR1-450****	N. rib 50' west of Amy fault, 450 Lv.	1 ^o	4	200°-206°	204°	4	7.8-8.1	7.9

Table 1 (continued)

Sample number	Location	Incls. type	Filling temperature (°C)			Salinity (equiv. wt. % NaCl)		
			No. Incls.	Temp. range	Mean temp.	No. Incls.	Saln. range	Mean saln.
AR4-450***	S. rib 90' west of Amy fault, 450 Lv.	p2°	9	219°-234°	228°	9	4.4-6.0	5.0
AR5-450**	W. rib, Amy fault drift, 450 Lv.	1° p2°	5 4	185°-202° 191°-215°	192°	5 4	4.9-11.2 7.5-7.8	6.6 7.7
AR15-450****	Face of west x-cut, 450 Lv.	1°	10	203°-237°	225°	-	-	-
AR16-450***	S. rib of x-cut 200' w. of Amy fault 450 Lv.	1° p2° 2°	16 15 7	190°-238° 210°-228° 202°-220°	206° 217° 209°	16 12 7	7.2-8.0 6.8-8.2 7.3-8.0	7.7 7.4 7.7
AR18-450***	S. rib of x-cut 186' w. of Amy fault 450 Lv.	1°	11	150°-221°	207°	10	6.8-7.2	6.9
AR19-450****	N. rib of x-cut 50' w. of "C" rse. 450 Lv.	1° p2°	5 6	153°-165° 195°-200°	159° 198°	5 6	4.9-8.4 7.5-7.8	7.4 7.7
AR21-450***	N. rib of x-cut 15' e. of Amy fault 450 Lv.	1°	6	200°-223°	220°	6	7.0-7.4	7.3
CM2-1****	Face of 50' x-cut, Comm. 2 Lv.	1° Clath. 2°	10 2 4	150°-205° 94°-125° 180°-193°	168° 110° 181°	11 - 4	5.5-8.5 6.1-7.0	6.0 6.5
CM2-3***	Face of 50' x-cut, Comm. 2 Lv.	1°	7	145°-179°	161°	7	4.3-5.4	4.6

Table 1 (continued)

Sample number	Location	Incls. type	Filling temperature (°C)			Salinity (equiv. wt. % NaCl)		
			No. Incls.	Temp. range	Mean temp.	No. Incls.	Saln. range	Mean saln.
CM2-6****	30' east of face in 50' x-cut, Comm.2 Lv.	l ^o	5	148 ^o -190 ^o	164 ^o	5	4.8-5.1	5.0
CM2-7***	25' east of face in 50' x-cut, Comm.2 Lv.	l ^o	5	165 ^o -178 ^o	170 ^o	5	5.8-7.5	6.1
CM2-4**	Near face of 50' x-cut, Comm. 2 Lv.	l ^o Clath. p2 ^o	4 2 9	151 ^o -183 ^o 98 ^o -131 ^o 141 ^o -194 ^o	164 ^o 115 ^o 169 ^o	4 2 5	5.0-6.3 3.8-4.4	5.6 4.2
CM2-16**	Near face of 30' x-cut, Comm. 2 Lv.	l ^o Clath.	9 2	175 ^o -202 ^o 154 ^o -187 ^o	189 ^o 170 ^o	9 2	5.0-5.6	5.3
BM710-360****	Core hole on Bach. Mtn., 360' @-60' east, 10451' el.	l ^o Clath. p2 ^o	7 2 5	158 ^o -191 ^o 171 ^o -265 ^o 152 ^o -190 ^o	166 ^o 218 ^o 180 ^o	7 2 5	6.5-8.0 6.1-8.5	7.0 6.6
CDS4-150***	Core hole on Bach. Mtn., 150' @-45' west, 10427' el.	l ^o p2 ^o	8 6	140 ^o -198 ^o 158 ^o -163 ^o	171 ^o 160 ^o	8 6	5.0-6.2 5.1-6.1	5.4 5.4
CDS4-629***	Core hole on Bach. Mtn., 629' @-45' west, 10093' el.	l ^o p2 ^o	6 7	197 ^o -210 ^o 188 ^o -216 ^o	205 ^o 205 ^o	6 7	7.6-8.0 6.8-10.2	7.8 7.4
CDS4-650***	Core hole on Bach. Mtn., 650' @-45' west, 10078' el.	l ^o p2 ^o	5 3	189 ^o -208 ^o 176 ^o -198 ^o	198 ^o 182 ^o	5 3	8.7-9.1 7.6-8.0	9.0 7.8

Table 1 (continued)

Sample number	Location	Incls. type	Filling Temperature (°C)			Salinity (equiv. wt. % NaCl)		
			No. Incls.	Temp. range	Mean temp.	No. Incls.	Saln. range	Mean Saln.
CDS4-920***	Core hole on Bach. Mtn. 920' @ 45° west, 9883' elevation	1° p2°	5 3	200°-244° 185°-190°	213° 188°	5 3	7.0-9.5 8.1-8.4	8.3 8.3

Table 2. Individual fluid inclusion data. All of these inclusions were included in table 1, but were not separated as individual inclusions. All of the inclusions plotted in fig. 6 are included in this table. It was not possible to obtain both homogenization temperature and salinity for every inclusion that was examined in this study.

Table 2. Individual Fluid Inclusion Data

Sample number	Elevation	Filling temperature (°C)	Salinity (equiv. wt. % NaCl)
AR16E	2844 m.	175 ⁰	7.0
AR16E	2844 m.	195 ⁰	7.1
AR16E	2844 m.	192 ⁰	7.5
AR16E	2844 m.	194 ⁰	7.9
AR16E	2844 m.	197 ⁰	9.6
AR16E	2844 m.	195 ⁰	7.1
AR16E	2844 m.	202 ⁰	7.5
AR16E	2844 m.	204 ⁰	9.0
AR16E	2844 m.	206 ⁰	9.4
AR16E	2844 m.	209 ⁰	9.5
AR16E	2844 m.	214 ⁰	6.8
AR16E	2844 m.	217 ⁰	7.2
AR12E	2844 m.	219 ⁰	8.5
AR12E	2844 m.	221 ⁰	6.0
AR12E	2844 m.	228 ⁰	7.6
AR2E	2844 m.	222 ⁰	9.8
AR2E	2844 m.	224 ⁰	7.4
AR2E	2844 m.	226 ⁰	7.8
AR2E	2844 m.	225 ⁰	10.0
AR2E	2844 m.	228 ⁰	10.0
AR2E	2844 m.	228 ⁰	9.8
AR2E	2844 m.	234 ⁰	6.3
AR2E	2844 m.	239 ⁰	6.3
AR2E	2844 m.	234 ⁰	6.4
AR2E	2844 m.	239 ⁰	6.3
AR2E	2844 m.	236 ⁰	6.7
AR2E	2844 m.	240 ⁰	6.8
AR2E	2844 m.	231 ⁰	6.8
AR2E	2844 m.	232 ⁰	7.3
AR2E	2844 m.	236 ⁰	9.7
AR2E	2844 m.	237 ⁰	9.7
AR2E	2844 m.	238 ⁰	9.9
AR2E	2844 m.	235 ⁰	9.8
AR2E	2844 m.	234 ⁰	9.8
AR2E	2844 m.	236 ⁰	9.8
AR2E	2844 m.	253 ⁰	6.7
AR2E	2844 m.	250 ⁰	7.0
AR2E	2844 m.	246 ⁰	9.9
AR1E	2844 m.	228 ⁰	7.2
AR1E	2844 m.	228 ⁰	7.4
AR1E	2844 m.	234 ⁰	5.7
AR1E	2844 m.	238 ⁰	5.7
AR1E	2844 m.	237 ⁰	7.0
AR1E	2844 m.	234 ⁰	7.2
AR1E	2844 m.	236 ⁰	12.9
AR1E	2844 m.	238 ⁰	12.8
AR1E	2844 m.	242 ⁰	12.8
AR20E	2844 m.	229 ⁰	7.8

Table 2 (continued)

Sample number	Elevation	Filling temperature (°C)	Salinity (equiv. wt. % NaCl)
AR20E	2844 m.	238°	8.0
AR20E	2844 m.	242°	8.1
AR20E	2844 m.	243°	7.8
AR20E	2844 m.	246°	7.8
AR13E	2844 m.	225°	8.0
AR13E	2844 m.	230°	9.3
AR13E	2844 m.	237°	9.3
AR13E	2844 m.	236°	9.5
AR13E	2844 m.	244°	9.0
AR13E	2844 m.	248°	9.4
AR13E	2844 m.	252°	9.0
AR24E	2844 m.	222°	9.1
AR24E	2844 m.	227°	9.0
AR24E	2844 m.	239°	8.5
AR24E	2844 m.	241°	8.8
AR24E	2844 m.	248°	9.0
AR24E	2844 m.	242°	9.2
AR24E	2844 m.	252°	9.0
AR24E	2844 m.	260°	8.9
AR4E	2844 m.	229°	10.0
AR4E	2844 m.	239°	10.1
AR4E	2844 m.	235°	10.3
AR4E	2844 m.	238°	10.6
AR4E	2844 m.	243°	10.0
AR15E	2844 m.	237°	8.8
AR15E	2844 m.	246°	8.6
AR15E	2844 m.	250°	8.8
AR14D	2880 m.	199°	7.4
AR14D	2880 m.	232°	8.0
AR14D	2880 m.	240°	9.0
AR14D	2880 m.	225°	7.5
AR5D	2880 m.	191°	7.4
AR5D	2880 m.	248°	10.2
AR5D	2880 m.	246°	10.2
AR5D	2880 m.	227°	9.0
AR5D	2880 m.	204°	9.0
AR13D	2880 m.	207°	6.5
AR13D	2880 m.	215°	6.5
AR13D	2880 m.	217°	6.4
AR11D	2880 m.	215°	5.7
AR11D	2880 m.	178°	3.7
AR11D	2880 m.	206°	5.0
AR11D	2880 m.	204°	5.2
AR11D	2880 m.	219°	5.8
AR11D	2880 m.	216°	4.9
AR11D	2880 m.	200°	5.0

Table 2 (continued)

Sample number	Elevation	Filling temperature (°C)	Salinity (equiv. wt. % NaCl)
AR11D	2880 m.	215°	5.8
AR10D	2880 m.	234°	7.0
AR10D	2880 m.	223°	6.1
AR10D	2880 m.	225°	6.1
AR10D	2880 m.	216°	6.1
AR10D	2880 m.	220°	6.0
AR10D	2880 m.	223°	6.3
AR10D	2880 m.	218°	6.4
AR10D	2880 m.	228°	6.8
AR10D	2880 m.	223°	6.8
AR10D	2880 m.	220°	6.0
AR10D	2880 m.	228°	7.5
AR10D	2880 m.	232°	7.4
AR10D	2880 m.	233°	7.4
AR10D	2880 m.	230°	6.3
AR10D	2880 m.	226°	6.2
AR1C	2904 m.	168°	8.4
AR1C	2904 m.	172°	9.7
AR1C	2904 m.	181°	9.6
AR1C	2904 m.	182°	10.1
AR1C	2904 m.	202°	9.3
AR1C	2904 m.	215°	6.6
AR1C	2904 m.	213°	10.1
AR1C	2904 m.	216°	10.2
AR2C	2904 m.	183°	7.4
AR2C	2904 m.	181°	8.2
AR2C	2904 m.	183°	7.2
AR2C	2904 m.	193°	7.7
AR2C	2904 m.	199°	8.3
AR2C	2904 m.	204°	8.8
AR2C	2904 m.	206°	8.2
AR2C	2904 m.	203°	7.9
AR2C	2904 m.	216°	8.6
AR2C	2904 m.	216°	8.9
AR2C	2904 m.	221°	7.2
AR2C	2904 m.	222°	9.0
AR2C	2904 m.	227°	7.2
AR2C	2904 m.	235°	7.2
AR2C	2904 m.	239°	7.5
AR3C	2904 m.	187°	7.4
AR3C	2904 m.	189°	7.3
AR3C	2904 m.	188°	6.8
AR3C	2904 m.	194°	7.9
AR3C	2904 m.	195°	7.6
AR3C	2904 m.	197°	7.6
AR3C	2904 m.	197°	7.4

Table 2 (continued)

Sample number	Elevation	Filling temperature (°C)	Salinity (equiv. wt. % NaCl)
AR3C	2904 m.	197°	7.7
AR3C	2904 m.	199°	7.6
AR3C	2904 m.	204°	7.5
AR3C	2904 m.	205°	5.9
AR4C	2904 m.	192°	7.4
AR4C	2904 m.	192°	7.8
AR4C	2904 m.	195°	7.8
AR4C	2904 m.	196°	7.9
AR4C	2904 m.	200°	7.9
AR4C	2904 m.	206°	7.9
AR4C	2904 m.	209°	7.8
AR4C	2904 m.	207°	5.6
AR4C	2904 m.	209°	6.3
AR4C	2904 m.	210°	6.8
AR4C	2904 m.	212°	6.3
AR4C	2904 m.	212°	5.9
AR4C	2904 m.	214°	6.1
AR4C	2904 m.	213°	5.6
CM2-1	3157 m.	153°	5.6
CM2-1	3157 m.	157°	5.7
CM2-1	3157 m.	181°	5.8
CM2-1	3157 m.	183°	6.1
CM2-1	3157 m.	183°	5.8
CM2-1	3157 m.	188°	6.8
CM2-1	3157 m.	192°	7.2
CM2-1	3157 m.	193°	6.8
CM2-1	3157 m.	194°	6.3
CM2-1	3157 m.	201°	7.2
CM2-3	3157 m.	146°	4.3
CM2-3	3157 m.	151°	5.4
CM2-3	3157 m.	155°	5.0
CM2-3	3157 m.	159°	5.4
CM2-3	3157 m.	164°	5.1
CM2-4	3157 m.	162°	5.5
CM2-4	3157 m.	164°	6.0
CM2-4	3157 m.	164°	5.8
CM2-4	3157 m.	188°	4.2
CM2-4	3157 m.	179°	4.2
CM2-6	3157 m.	150°	5.1
CM2-6	3157 m.	153°	5.1
CM2-7	3157 m.	168°	5.4
CM2-7	3157 m.	174°	5.5
CM2-7	3157 m.	178°	7.4
CM2-7	3157 m.	178°	6.0
CM2-16	3157 m.	177°	5.6

Table 2 (continued)

Sample number	Elevation	Filling temperature (°C)	Salinity (equiv. wt. % NaCl)
CM2-16	3157 m.	179°	5.4
CM2-16	3157 m.	183°	5.6
CDS4-150	3178 m.	152°	3.9
CDS4-150	3178 m.	148°	4.6
CDS4-150	3178 m.	152°	4.6
CDS4-150	3178 m.	157°	4.7
CDS4-150	3178 m.	158°	4.9
CDS4-150	3178 m.	162°	4.8
CDS4-150	3178 m.	162°	5.0
CDS4-150	3178 m.	155°	5.1
CDS4-150	3178 m.	158°	5.2
CDS4-150	3178 m.	160°	5.6
CDS4-150	3178 m.	158°	6.9
CDS4-150	3178 m.	154°	5.6
BM71C-360	3185 m.	181°	5.4
BM71C-360	3185 m.	184°	5.5
BM71C-360	3185 m.	186°	5.7
BM71C-360	3185 m.	182°	5.8
BM71C-360	3185 m.	191°	5.6
BM71C-360	3185 m.	190°	5.9
BM71C-360	3185 m.	196°	5.9
BM71C-360	3185 m.	185°	6.0
BM71C-360	3185 m.	188°	6.1

APPENDIX B

Comparison of Creede to Other Geothermal Systems

The idea that Creede may be a fossil geothermal system was treated in detail by Wetlaufer and others (1978). Data obtained in this study add more evidence to this idea and more comparisons to other geothermal systems, both active and fossil, are thus needed. Ore depositional models with many similar aspects have been proposed for the Creede district by several authors (Steven and Eaton, 1975; Bethke and others, 1976; Barton and others, 1977; Bethke and Rye, 1979; and Giudice, 1980). These models are based on a variety of geologic and geochemical evidence that has been integrated into a proposed complex hydrologic system that is summarized below.

Barton et.al. (1977) proposed a model of ore deposition based on fluid inclusion data, mineralogy and paragenesis of the ores, zoning of the minerals, and the location of zones of hydrothermal leaching. They postulated that a large deeply circulating hydrothermal system composed of hot (250°C) and moderately saline (<12 wt. %) fluids rose from depth and entered the vein system in the north. These fluids then flowed to the south at approx. 500 to 1000 m below the surface, precipitating ore and gangue minerals along their path. At places some of the ore and gangue minerals were leached by these same fluids. The fluids cooled as they flowed south and were boiling at times

along the top of the cell. As the fluids reached the southern end of the vein system they encountered the ring fracture system of the Creede caldera and most of the fluids were convected back downward. Some of these fluids are thought to have reached the surface along the faults or through the porous sediments of the Creede formation. After again descending the fluids were reheated at depth and recharged in metals, sulfur, silica, etc., before again ascending to repeat the cycle. Doe et.al. (1979) determined through lead isotope data that the source of the lead in the Creede district to be the Precambrian rocks that are believed to underlie the volcanics in the area. The source of the fluids was determined through stable isotope studies by Bethke and Rye (1979) to have both meteoric and magmatic constituents, as has been the case at several other deposits also, White (1974). The magmatic fluid is thought to have been of importance during carbonate deposition, while most of the sulfide minerals and quartz were deposited by meteoric waters that had two different isotopic signatures indicating different reservoirs. All three waters are believed to have been present episodically in the hydrothermal system at different times during the lifespan of the system and only limited amounts of interaction between the different waters occurred.

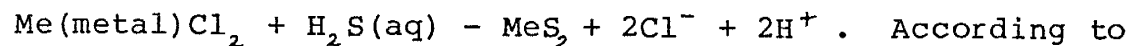
The data presented in this study also supports that lateral flow along the top of the cell occurred as in the model presented above. Wetlaufer et.al. (1978) suggest

also that two cells may have existed during mineralization at Creede; the deeply circulating cell described above along with a more dilute shallow shallow system. An examination of other geothermal systems, both active and fossil, shows that several authors have also proposed stacked, or multi-tiered, models for several geothermal areas (Sorey et.al., 1978; Elder, 1965; Fournier, 1979; Sigvaldson and Cuellar, 1971; Grose, 1977; Ellis and Mahon, 1977; Nakamura et.al., 1971). The significance of stacked geothermal cells is in the controls of ore deposition and zonation that is expected from the interaction of hot saline solution below and and the dilute cooler solution from near the surface.

The presence of metals in solution has been observed in several active hydrothermal systems. The thermal pools in New Zealand (Ellis, 1969), the Red Sea brines (Shanks and Bischoff, 1977), the Salton Sea brines (Skinner et.al., 1967), waters from Steamboat Springs, Nevada (White, 1968), and waters from several Japanese hot springs (Uzumasa, 1965) all have relatively high amounts of metals in solution when compared to normal groundwater solutions. The form in which these metals are transported in solution has been determined to be as chloride, fluoride, sulfide, ammonia, and organic complexes, with chloride and sulfide complexes as by far the most common (Barnes, 1979; Seward, 1976; Ellis, 1979; Weissberg et.al., 1979; Helgeson, 1964; Barnes and Czmanske; 1967, White, 1968; Ewers and Keays, 1977;

Barton et.al., 1977). At Creede Barton et.al. (1977) believes that metals were most likely transported in chloride complexes. These authors also determined the concentration of sulfur species in solutions contained in fluid inclusions from the OH vein to be 0.02 molal compared to 1.0 molal Cl^- in solution, so that their assumption of metal-chloride complexes seems valid.

Precipitation of metal-chloride complexes from solution may be represented by the following general equation:



Barnes (1979) the following mechanisms can cause precipitation from this type of reaction: 1) increased concentration of sulfur (H_2S in this case) in solution; 2) increased pH; 3) decreased chloride concentration, due to dilution by circulating meteoric water; 4) decreased temperature which lowers the solubility coefficients; or by 5) reducing the amount of oxygen. In the environment of ore deposition that was present at Creede all of these mechanisms probably contributed in various degrees to precipitation of metals from solution. Norman et.al., (1976) conclude that the oxidation of hydrothermal fluids can cause ore precipitation, but the amount of precipitation due to oxidation at Creede is unknown. The presence of hypogene oxides (hematite, pyrolusite, and other Mn-oxides) in the upper levels of the mine near the southern end of the system indicates that oxidation may have been a significant factor in causing precipitation on a local scale if at least

some of the iron and manganese was transported as a sulfide complex. The other factors mentioned above have all been mentioned as important controls in ore deposition in several hydrothermal deposits.

Buchanan (1980) found that a major control of ore deposition at Guanajuato, Mexico was boiling of the ore fluid causing a rise in pH, cooling of the remaining fluid, and a rise in the oxygen fugacity. White (1955, 1967), Ewers and Keays (1977), and Casadevall and Ohmoto (1977) believe that cooling and pH (controlled by boiling and/or temperature decrease) are the major controls of ore deposition in the deposits that they studied. Ellis (1969), Helgeson (1964), and Ellis and Mahon (1977) all conclude that salinity and/or temperature are the most significant factors in precipitation in the deposits which they studied. In several geothermal areas the limiting factor in precipitation of sulfide minerals is not the amount of metal in solution, but rather it is the amount of sulfur species, (Weissberg et.al., 1979). The solutions analyzed from fluid inclusions at Creede by Czmanske et.al. (1963) shows that the concentration of metals in these solutions is much higher than concentrations in fluids from several active geothermal systems where sulfides are found at intermediate depths, such as at Broadlands and other areas, Ellis (1969). Ore deposition in the OH vein was found by Barton et.al. (1977) to be the result of gradual cooling of the ore fluids and boiling near the top of the system. In the model that

they support Wetlaufer et.al. (1978) state that the saline, deeply circulating hydrothermal cell responsible for ore transport and deposition was most likely separated from any dilute shallow system that may have existed. The top of OH vein mineralization is marked by an extensive zone of sericitic alteration that appears to occur over almost the entire vein. This alteration capping is analogous to impermeable "cap" rocks found in many geothermal systems as noted by Ellis (1979) and Helgeson (1968). These "cap" rocks prevent rapid outflow from the convection system, and cause lateral flow of water beneath the impermeable layer. Although the sericite alteration "cap" that is present over much of the Creede system may not have formed a seal (due to continuous minor movement of faults during mineralization) to confine the solutions below, it certainly would have promoted lateral flow of the deeper solutions and prevented most interaction of the deep hydrothermal fluids with shallow circulating fluids. Fluid inclusions showing evidence of boiling from the upper portions of the OH vein indicate temperatures of approx. 250°C for boiling, and data from Haas (1971) reveals that the water depth necessary to restrain boiling to this temperature to be approx. 500 meters. Although no evidence was found in the fluid inclusions in the present study that can be taken as proof that boiling took place as was found on the OH vein, evidence of high amounts of CO₂ and/or CH₄ found in several inclusions from the upper levels of the study area that are

taken as indirect indications that boiling may have occurred. The homogenization temperatures in these inclusions were in the range 170° to 175°c. Again from data in Haas (1971,1976) the depth of water necessary to restrain boiling to this temperature is approx. 90 meters. Only a very limited amount of intense sericitic alteration (similar to that found in the OH area) has been found near the southern end of the Amethyst system indicating that perhaps very little boiling occurred in this area and that there was no impermeable "cap" over the ore solutions to prevent interaction of deep and shallow solutions. Therefore dilution and more rapid temperature decrease due to mixing solutions may have had a greater influence on sulfide precipitation in the current study area than they did in the OH vein.

As presented previously, homogenization temperatures from fluid inclusions in the study area increased with depth. This is also reported to be true at Broadlands (Ellis, 1979). At several active geothermal areas, including Broadlands, there have been sulfides found in drill core and cuttings from intermediate depths according to Browne (1969). In the upper portions of the study area, where nearly all of the temperatures were below 185c, very few sulfides were found, but in the lower workings (temperatures above 220°c) there were abundant sulfides present. The fact that salinities also increase with depth in the study area indicates that mixing may have occurred.

Also discussed previously is that at Creede broad vertical and horizontal zones of disseminated mineralization were deposited at depths of 150 to 400 meters below the surface at the time of deposition. These depths are shallower than the level where base-metal and Ag sulfides were found at Broadlands (Ewers and Keays, 1977; Weissberg et.al., 1979). Wetlaufer et.al. (1978) conclude that the major characteristics of the Creede deposit are similar in many respects to those found in many in active geothermal systems. The fluid inclusion and mineralogical evidence from this study add support to the idea that Creede may be a fossil geothermal system, although questions concerning the relatively shallow depth zonation of the mineralization at Creede compared to depth zonation in several active geothermal systems remain unanswered.

REFERENCES

- Arangano, E. E., Buitrago, J. A., Cataldi, R., Ferrare, G. C., Panichi, C., Villegas, J. V., 1971, Preliminary study on the Ruiz geothermal project (Colombia): UN Symposium on the Development and Utilization of Geothermal Resources, Pisa, 1970, Pr. (Geothermics, Spec. Iss. 2), v. 2, pt.1, p. 43-56
- Barnes, H. L., 1979, Solubilities of ore minerals, in Barnes, H. L., ed., Geochemistry of hydrothermal ore deposits: 2nd ed., John Wiley and Sons, Inc., p. 404-460
- Barnes, H. L., and Czmanske, G. K., 1967, Solubilities and transport of ore minerals, in Barnes, H. L., ed., Geochemistry of hydrothermal ore deposits: New York, Holt, Rinehart, and Winston, p. 334-381
- Barton, P. B., Bethke, P. B., Roedder, Edwin, 1977, Environment of ore deposition in the Creede mining district, San Juan Mountains, Colorado: Part III: Progress toward interpretation of the chemistry of the ore forming fluid; Econ. Geol., v. 72, 24 p.
- Barton, P. B. Jr., Bethke, P. M., and Toulmin, M. S., 1971, An attempt to determine the vertical component of flow rate of ore forming solutions in the OH vein, Creede, Colorado; Soc. Min. Geol. Japan Spec. Iss. 2, p. 132-136
- Bethke, P. M., and Barton, P. B. Jr., 1971, History of filling of the OH vein, Creede, Colorado [abs]; Econ. Geol., v. 66, p.1265
- Bethke, P. M., Barton, P. B. Jr., and Bodine, M. W. Jr., 1960, Time space relationships of the ores at Creede, Colorado [abs], GSA Bull. v. 71, no. 12, pt.2, p. 1825-1826
- Bethke, Philip M., Barton, Paul B, Lanphere, Marvin A., and Steven, Thomas A., 1976, Environment of ore deposition in the Creede mining district, San Juan Mountains, Colorado : Part II: Age of mineralization; Econ. Geol., v. 71, p. 1006-1011

- Bethke, P. M., Rye, R. O., and Barton, P. B., 1973, Hydrogen, oxygen, and sulfur isotopic compositions of ore fluids in the Creede district, Mineral County, Colorado [abs]; *Econ. Geol.*, v. 68, p.1205
- Bethke, P. M., and Rye, R. O., 1979, Environment of ore deposition in the Creede mining district, San Juan mountains, Colorado: Part IV. Source of fluids from oxygen, hydrogen, and carbon isotope studies; *Econ. Geol.*, vol. 74, p. 1832-1851
- Browne, P. R. L., 1969, Broadlands geothermal drill hole, Tampo Volcanic Zone, New Zealand; *Econ. Geol.*, v. 64, p. 156-159
- Buchanan, L. J., 1980, Ore controls of vertically stacked deposits, Guanajuato, Mexico; Preprint for AIME Annual Meeting, 26 p.
- Casadevall, T., and Ohmoto, H., 1977, Sunnyside Mine, Eureka mining district, San Juan County, Colorado: geochemistry of base and precious metal ore deposition in a volcanic environment: *Econ. Geol.*, v.72, p. 1285-1320
- Collins, Peter L., 1979, Gas hydrates in CO₂-bearing fluid inclusions and the use of freezing data for estimation of salinity; *Econ. Geol.*, v. 74, p. 1435-1444
- Czmanske, G. K., Roedder, E., and Burns, F. C., 1963, Neutron activation analysis of fluid inclusions for copper, manganese, and zinc; *Science*, v. 140, p. 401-403
- Doe, B. R., Steven, T. A., Delevaux, M. H., Stacey, J. S., Lipman, P. W., and Fisher, F. S., 1979, Genesis of ore deposits in the San Juan volcanic field southwestern Colorado; *Econ. Geol.*, v. 74. p. 1-26
- Edwards, A. B., 1947, Textures of the Ore Minerals; Brown, Prior, Anderson Pty., Australia, 242 p.
- Elder, J. W., 1965, Physical processes in geothermal areas, in *Terrestrial Heat Flow: Geoph. Mon. 8*, NAS-NRC No. 128, Am. Geophys. Union, p. 211-239

- Ellis, A. J., 1969, Present day hydrothermal systems and mineral deposition: in Ninth Commonwealth Mining and Metallurgical Congress 1969, London, Paper 7, 30 p.
- Ellis, A. J., 1979, Explored geothermal systems: in Barnes, H. L., ed., Geochemistry of Hydrothermal Ore Deposits: New York, John Wiley and Sons, Inc., p. 632-683
- Ellis, A. J., and Mahon, W. A. J., 1977, Chemistry and Geothermal Systems: Academic Press, New York, 392 p.
- Emmons, W. H., and Larsen, E. S., 1913, A preliminary report on the geology and ore deposits of Creede, Colorado: U. S. Geol. Survey Bull. 530
- _____, 1923, Geology and ore deposits of the Creede district, Colorado: U. S. Geol. Survey Bull. 718
- Ewers, J. R., and Keays, R. R., 1977, Volatile and precious metal zoning in the Broadlands geothermal field, New Zealand: Econ. Geol., v. 72, p. 1337-1354
- Fournier, R. O., 1979, Geochemical and hydrologic considerations and the use of enthalpy-chloride diagrams in the predictions of underground conditions in hot-spring systems: Jour. of Volc. and Geothermal Research, v. 5, p.1-16
- Fournier, R. O., and Truesdell, A. H., 1974, Geochemical indicators of subsurface temperature- Part 2. Estimation of temperature and fraction of hot water mixed with cold water; U. S. Geol. Survey Jour. Res., v. 2, p. 263-269
- Giudice, P. M., 1980, Mineralization at the convergence of the Amethyst and OH fault systems, Creede district, Mineral County, Colorado; MSc. Thesis, Univ. of Arizona, 95 p.
- Grose, L. T., 1977, Subsurface geology in geothermal systems: in Subsurface Geology, editors L. W. LeRoy, D. O. LeRoy, and J. W. Raese; Colo. School of Mines Pub., Golden, Colorado

- Haas, John L., 1971, The effect of salinity on the maximum thermal gradient of a hydrothermal system at hydrostatic pressure: *Econ. Geol.*, v. 66, p. 940-946
- Haas, J. L., Jr., 1976, Thermodynamic properties of the coexisting phases and thermochemical properties of the H₂O component in boiling solutions: *U. S. Geol. Survey Bull.* 1421-A
- Haas, J. L., and Potter, R. W., 1977, The measurement and evaluation of PTVX properties of geothermal brines and the derived thermodynamic properties: *Proceed. of the 7th Symp. on Thermophysical Properties*, p. 604-614
- Helgeson, H. C., 1964, *Complexing and hydrothermal ore deposition*: New York, Macmillan Co., 128 p.
- Helgeson, H. C., 1968, Geologic and thermodynamic characteristics of the Salton Sea geothermal system; *Am. Jour. Science*, v. 266, p. 129-166
- Hull, D. A., 1970, *Geology of the Puzzle Vein, Creede mining district, Colorado*: Ph.D. Dissertation, Univ. of Nevada
- Kelly, William C., and Rye, Robert O., 1979, Geologic, fluid inclusion, and stable isotope studies of the tin-tungsten deposits of Panasqueira, Portugal; *Econ. Geol.*, v. 74, p. 1721-1822
- Larsen, E. S., 1929, *Recent developments in the Creede district, Colorado*: *U. S. Geol. Survey Bull.* 811-B
- Lipman, P. W., Steven, T. A., and Mehnert, H. H., 1970, Volcanic history of the San Juan Mountains, Colorado, as indicated by potassium-argon dating; *Geol. Soc. America Bull.*, v. 81, p. 2329-2352

- Nakamura, H., Sumi, K., Katigiri, K., and Jwata, T., 1971, The geological environment of Matsukawa Geothermal Area, Japan: U. N. Symposium of the Development and Utilization of Geothermal Resources, Pisa., 1970, Pr. (Geothermics, Spec. Iss. 2), v. 2, pt. 1, p. 221-223
- Noguchi, T., Nishikawa, K., Ito, T., and Ushijima, K., 1971, Some theoretical considerations on hydrothermal systems due to cracks: U. N. Symposium on the Developments and Utilization of Geothermal Resources, Pisa, Pr. (Geothermics, Spec. Iss. 2), v. 2, pt. 1, p. 655-666
- Norman, D. I., 1977, Geology and geochemistry of the Tribag Mine, Batchawana Bay, Ontario; Ph.D. Thesis, Univ. of Minnesota, 251p.
- Norman, D. I., Landis, G. P., and Sawkins, F. J., 1976, H₂S and SO₂ in fluid inclusions (abs); Geol. Soc. America, Abs. Program, 8, p. 1031
- Norton, D., and Cathles, L. M., 1979, Thermal aspects of ore deposition; in Barnes, H. L., Geochemistry of hydrothermal ore deposits, 2nd ed., New York, John Wiley and Sons, Inc., p. 611-631
- Ratte, J. C., and Steven, T. A., 1967, Ash flows and related volcanic rocks, associated with the Creede caldera, San Juan Mountains, Colorado: U. S. Geol. Survey Prof. Paper 524-H
- Roedder, Edwin, 1960, Primary fluid inclusions in sphalerite crystals from the OH vein; Creede, Colorado: Geol. Soc. America Bull., v. 71, no. 12, p. 1958
- _____, 1967, Metastable superheated ice in liquid-water inclusions under high negative pressure; Science, v. 155, p. 1413-1417
- _____, 1974, Changes in ore fluids with time, from fluid inclusion studies at Creede, Colorado: 4th Symp. Int. Assoc. on Genesis of Ore Deposits, Varna, 1974, v. II, p. 179-185

- Rye, R. O., and Sawkins, F. J., 1974, Fluid inclusion and stable isotope study on the Casapalca As-Pb-Zn-Cu deposit, Central Andes, Peru; *Econ. Geol.*, v.69, p. 181-205
- Seward, T. M., 1976, The stability of chloride complexes of silver in hydrothermal solutions up to 350°C; *Geochim. Cosmochim. Acta*, v. 40, p. 1329-1341
- Shanks, W. C., III, and Bischoff, J. L., 1977, Ore transport and deposition in the Red Sea geothermal system; a geochemical model: *Geochim. et. Cosmochim. Acta*, v. 41, p. 1505-1519
- Sigvaldson, G. E., and Cuellar, G., 1971, Geochemistry of the Ahuachapan thermal area, El Salvador, Central America: U. N. Symposium of the Development and Utilization of Geothermal Resources, Pisa, 1970, Pr. (Geothermics, Spec. Iss. 2), v. 2, pt. 1, p. 1392-1413
- Skinner, B. J., White, D. E., Rose, H. J., and Mays, R. E., 1967, Sulfides associated with the Salton Sea geothermal brine: *Econ. Geol.*, v. 62, p. 316-330
- Sorey, M.L., Lewis, R. E., and Olmsted, F. H., 1978, The hydrothermal system of Long Valley caldera, California: *U. S. Geol. Survey Prof. Paper 1044-A*
- Steven, T. A., 1975, Middle Tertiary volcanic field in the southern Rocky Mountains: *Geol. Soc. America Mem.* 144, p. pp75-94
- Steven, T. A., and Eaton, G. P., 1975, Environment of ore deposition in the Creede mining district, San Juan Mountains, Colorado; I. Geologic, hydrologic, and geophysical setting: *Econ. Geol.*, v.70, p.1023-1037
- Steven, T. A., and Epis, R. C., 1968, Oligocene volcanism in south-central Colorado; in Epis, R. C., ed., *Colorado School of Mines Quart.*, v. 63, p. 241-258
- Steven. T. A., and Lipman, P. W., 1976, Calderas of the San Juan volcanic field, southwestern Colorado: *U. S. Geol. Survey Prof. Paper 958*, 35 p.

- Steven, T. A., and Ratte, J. C., 1960, Relation of mineralization to caldera subsidence in the Creede district, San Juan Mountains, Colorado: U. S. Prof. Paper 400-B, p. B14-B17
- Steven, T. A., and Ratte, J. C., 1965, Geology and structural control of ore deposition in the Creede district, San Juan Mountains, Colorado: U. S. Geol. Survey Prof. Paper 487
- Truesdell, A. H., and Fournier, R. O., 1976, Calculation of deep temperatures in geothermal systems from the chemistry of boiling spring waters of mixed origin; 2nd UN Symposium on the Development and Use of Geothermal Resources, Pr., San Francisco, 1975, v. 1, p. 837-844
- Uzumasa, Y., 1965, Chemical investigations of hot springs in Japan; Tokyo, Tsukiji Shokan Co. LTD., 188 p.
- Weissberg, B. G., Browne, P. R. L., and Seward, T. M., 1979, Ore metals in active geothermal systems, in Barnes, H. L., ed., Geochemistry of hydrothermal ore deposits: 2nd ed., New York, John Wiley and Sons, Inc., p. 738-780
- Wetlaufer, P. H., 1977, Geochemistry and mineralogy of the carbonates of the Creede mining district, Colorado: U. S. Geol. Survey Open-file Report, p. 77-706
- Wetlaufer, P. H., Behtke, P. M., Barton, P. B., and Rye, R. O., 1978, The Creede Ag-Pb-Zn-Cu-Au district, central San Juan Mountains, Colorado: a fossil geothermal system: Nev. Bureau of Mines and Geol. Report 33, p. 159-164
- White, D. E., 1955, Thermal springs and epithermal ore deposits: Econ. Geol. 50th Anniv. Vol., p. 99-154
- White, D. E., 1967, Mercury and base-metal deposits with associated thermal and mineral waters, in Barnes, H. L., ed., Geochemistry of hydrothermal ore deposits: 1st ed., Holt, Rinehart, and Winston, NY, p. 575-631

White, D. E., 1968, Hydrology, activity, and heat flow of the Steamboat Springs thermal area, Washoe county, Nevada: U. S. Geol. Survey Prof Paper 458-C

White, D. E., 1974, Diverse origins of hydrothermal ore fluids: Econ. Geol., v. 69, p.954-973

This thesis is accepted on behalf of the faculty of the

Institute by the following committee:

David A. Norman
Adviser

Philip M. Kottke

Max W. Bodine, Jr.

2 May 1981
Date